AN ABSTRACT OF THESIS OF

Philip Jensen for the degree of Master of Science in Nuclear Engineering presented on March 8, 2013.

Title: Application of Sandwich Structure Analysis in Predicting Critical Flow Velocity for a Laminated Flat Plate

Abstract approved:_____

Wade R. Marcum

The Oregon State University (OSU), Hydro Mechanical Fuel test Facility (HMFTF) is designed to hydro-mechanically test prototypical plate type fuel. OSU's fuel test program is a part of the Global Threat Reduction Initiative (GTRI), formerly known as the Reduced Enrichment for Research and Test Reactor program. One of the GTRI's goals is to convert all civilian research, and test reactors in the United State from highly enriched uranium (HEU) to a low enriched uranium (LEU) fuel in an effort to reduce nuclear proliferation.

An analytical model has been developed and is described in detail which complements the experimental work being performed by the OSU HMFTF, and advances the science of hydro-mechanics. This study investigates two methods for determining the critical flow velocity for a pair of laminated plates. The objective is accomplished by incorporating a flexural rigidity term into the formulation of critical flow velocity originally derived by Miller, and employing sandwich structure theory to determine the rigidity term. The final outcome of this study results in the developing of a single equation for each of three different edge boundary conditions which reliably and comprehensively predicts the onset of plate collapse. The two models developed and presented, are termed the monocoque analogy and the ideal laminate model.

Application of Sandwich Structure Analysis in Predicting Critical Flow Velocity for a Laminated Flat Plate

by

Philip Jensen

A THESIS

Submitted to

Oregon State University

in partial fulfillment of

the requirements for the

degree of

Master of Science

Presented March 8, 2013

Commencement June 2013

Master of Science thesis of Philip Jensen presented on March 8, 2013.

APPROVED:

_____

Major Professor, representing Nuclear Engineering

_____

Head of the Department of Nuclear Engineering and Radiation Health Physics

_____

Dean of the Graduate School

I understand that my thesis will become part of the permanent collection of Oregon State University libraries. My signature below authorizes release of my thesis to any reader upon request.

_____

Philip Jensen, Author

ACKNOWLEDGEMENTS

To all of my family, friends, colleagues, and advisors…thanks for all of the help!

I would also like to thank the Department of Energy National Nuclear Security Administration and the Global Threat Reduction Initiative for funding my Graduate Research Assistantship at Oregon State University.

TABLE OF CONTENTS

TABLE OF CONTENTS (CONTINUED)

Section Page

LIST OF FIGURES

Figure Page

LIST OF TABLES

Table Page

Application of Sandwich Structure Analysis in Predicting Critical Flow Velocity for a Laminated Flat Plate

1 INTRODUCTION

The Oregon State University (OSU), Hydro Mechanical Fuel test Facility (HMFTF) is designed to test prototypical plate type fuel [1]. OSU's fuel test program is a part of the Global Threat Reduction Initiative (GTRI), formerly known as the Reduced Enrichment for Research and Test Reactor program. One of the GTRI's goals is to convert all civilian research, and test reactors in the United State from highly enriched uranium (HEU) to a low enriched uranium (LEU) fuel in an effort to reduce nuclear proliferation [2–4]. Although, numerous reactors have converted their fuel throughout the United States, several test reactors are designed in a manner which prevents them from converting to low enriched uranium using previously qualified fuel [5],[6]. This is because the reactors in questions operate with high power densities; they are referred to as High Performance Research Reactors (HPRR). The OSU HMFTF is in the process of experimentally evaluating a proposed LEU fuel under hydro-mechanical load. The proposed fuel is a laminated composite flat plate with Aluminum (Al) clad, and monolithic Uranium-Molybdenum (U-Mo) alloy core, which is in contrast to uranium aluminum dispersion fuel currently used [7]; cross-sectional sketches show the difference between the two in Figure 1-1.

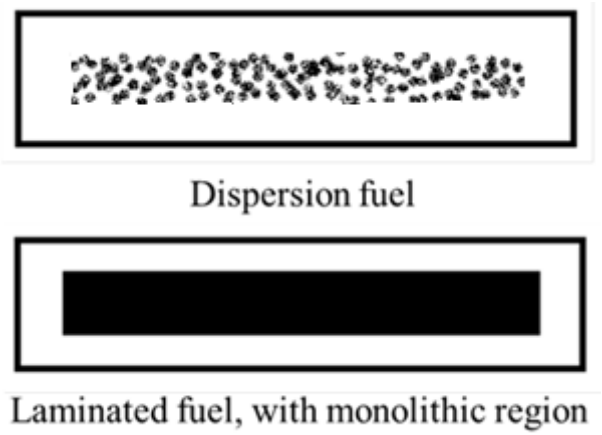

Figure 1-1: Cross-section of dispersion and laminated plate fuel

The HPRRs use a unique plate-type fuel geometry which promotes neutron efficiency and high power densities, however flat thin fuel plates tend to be mechanically weak under certain hydraulic conditions [8]. This weakness requires design criteria which identifies conditions in which fuel plates of a certain form are susceptible to mechanical 'failure'. Failure as defined by the HMFTF test plan, is the 'onset of plastic deformation' [7], this is in contrast to 'clad breach' which is typically defined as fuel failure [9],[10]. Prior work in plate fuel resulted in numerous flow metrics for predicting the hydro-mechanical stability of a plate under static and dynamic conditions [11–15]. Specifically, flow metrics that predict the static stability limits for fuels plates have traditionally focused on predicting the maximum flow rate, known as critical fluid velocity (originally derived by D.R. Miller [11]), across a plate which causes 'plate collapse' [11],[16]. Work has also been done which presents this critical flow velocity in terms of critical dynamic pressure [12].

'Plate collapse' is considered mechanical failure in these studies, and is a term that is left without specific a definition. For the sake of this study it can also be thought of as failure, and implies that the plate has deflected to such an extent that a linearized beam deflection model is no longer acceptable to characterize the phenomena at hand [13]. Such large deflections falls out of the applicability of the linearized method

proposed in Miller's original work, but also disallows the use of fundamentals tools such as the Euler-Bernoulli beam equation which requires small deflections [17–19]. The work presented herein utilizes the linearized method suggested by Miller and the Euler-Bernoulli beam equation therefore it is assumed to be valid up to, but not beyond the point of plate collapse.

1.1 Purpose

Previous work has shown the effectiveness of flow metrics such as the critical flow velocity predicted by Miller's model, for already qualified and currently deployed plate type fuel [20]. However, at this time little theoretical work has been done toward the development of a critical flow velocity model for laminated plate fuel.

The laminated fuel plates in question, are constructed with three discrete layers [21]. The inner layer is the U-Mo fueled region, and the outer two layers are the aluminum cladding. Structures comprised of three discrete laminated regions encompass a class of structures studied in composites known as 'sandwich structures' [22–24]. For this study, isotropic sandwich structure theory is adapted to critical flow velocity and critical dynamic pressure. This is because sandwich structure theory deals with each region, and quantifies how the three regions interact and contribute to the overall stiffness of the structure [22],[23],[25].

A method must be employed that applies sandwich structure theory to critical flow velocity and critical dynamic pressure, to the application of safety analysis for reactors using plate type fuel with three discrete layers.

1.2 Objectives

This study develops a flow metric that predicts a fluid's velocity, necessary to induce static mechanical instability of a plate undergoing hydraulic loading. This is referred to as critical flow velocity or critical dynamic pressure. It specifically caters to axial fluid flow over a flat laminated plate with two adjacent channels having fluid passing

through them. To accomplish this objective, the following tasks have been performed and are comprehensively described throughout this text:

- Identify existing methods used to estimate and predict the onset of plastic deformation in flat plates under isothermal hydraulic loading.

- Develop a model which characterizes the static deflection of a flat laminate plate when exposed to hydraulic loading while considering a variety of plate edge boundary conditions.

    - Identify parameters which characterize mechanical and hydraulic domain.

    - Create a mathematical relationship which correlates the influence of hydraulic pressure found in the fluid domain to that of the elastic response of a flat laminate plate in the mechanical domain.

- Employ the newly developed model under a set of test case conditions, and compare the outcomes against those produced with existing theoretical models.

- Identify and address, through discussion, observed discrepancies that arise between the newly developed flow metric for laminated plates, empirical data taken for these kinds of plates, and the existing metrics.

1.3 Document Overview

This document is organized in the following manner:

Chapter 1: Introduction – Introduction to the problem addressed by this thesis, motivation behind this thesis, and several tasks that have been addressed prior to completion of this thesis.

Chapter 2: Survey of Literature – Background information, a survey of previous works in flow induced deflection, a survey of previous work on sandwich structure analysis, and presenting previous work appropriate for comparison to the models developed in this thesis.

Chapter 3: Model and Methodology – Detailed description of the application of sandwich structure theory to critical flow velocity and critical dynamic pressure. Critical flow velocity and critical dynamic pressure are derived in this chapter, for three plate boundary conditions. Also, two methods for the derivation of plate flexural rigidity are presented.

Chapter 4: Results and Discussion – Comparison of the models developed in this thesis to three test cases, discussion of the applicability of these test cases, and discussion of the overall applicability to these test cases.

Chapter 5: Conclusion – Concluding remarks concerning this thesis.

Appendices, references, and a list of variables are provided at the end of this document for the reader's convenience.

2 SURVEY OF LITERATURE

This survey of literature is broken into two sections. The first section surveys work on hydro-mechanical stability of plates under axial flow conditions. The second section surveys work on the mechanics of laminated plates.

2.1 Flow induced deflection of plates

Flow induced deflections, and vibrations of flat plates has been studied by numerous authors. This is primarily because the flat plate geometry is mechanically weaker than other fuel plate geometries (i.e. cylindrical, involute) [15].

One of the first studies concerning fuel plates and flow induced phenomena was done by Stromquist and Sisman [26]. They created one of the first experimental facilities dedicated to studying flow induced instability of reactor fuel plates, and tested curved and flat plates. They were able to measure pressure drop through their test element, frequency, and amplitude of the observed vibrations. Also noted was "buckling" of fuel plates, due to a pressure difference between flow channels. This reference to buckling was one of the first references to what has become known as plate collapse. Stomquist and Sissman concluded that the plates they tested were of "adequate strength" to withstand the vibrational phenomena measured. Also, they made very useful observations noting that channel dimensions, edge clamping conditions, and manufacturing defects (e.g. brazing defects) contributed to the occurrence of the buckling phenomena.

Following Stomquist and Sissman, Doan published a report on technical issues that arose during the initial operation of the Engineering Test Reactor in 1958 [27]. In this report Doan, noted that a pressure differential was formed between two adjacent flow channels which drove plate instability. Also listed were a number of proposed modifications to the reactor's fuel to mitigate these effects.

In 1958 Miller published his work which set about creating a formula to predict the critical flow velocity that causes "plate collapse" [11]. Miller's work is important because it represents the first and most replicated attempt to quantify critical flow velocity. Miller studied both flat and curved plates, and devised a theoretical prediction for critical flow velocity by pairing fluid mechanics with solid mechanics. He approached the solid domain by noting that deflection of a plate is caused by a distributed force on its surface. This distributed force is analogues to the pressure difference that arises between two adjacent flow channels, developed within the fluid domain. Knowing this, the plate deflection can be quantified using the Euler-Bernoulli beam equation in conjunction with the wide beam approximation. This deflection is then used to find the relative distortion of the flow channel. Bernoulli's equation is then linearized, the velocity change between two adjacent channels due to plate deflection is noted, and the critical flow velocity is solved for[1]. This pairing of the fluid domain with the solid domain is important, because it showed that hydro-mechanical stability of plates is not exclusively dependent on the hydraulic conditions but also the solid mechanical conditions. This critical flow velocity is denoted as "Miller's velocity" by some authors. Although Miller developed a new and useful model for predicting plate buckling under hydraulic loading, a significant number of assumptions were required.

For flat plates, Miller assumed [11],[12]:

- The plate is isotropic, homogenous, linearly elastic, initially un-deformed and perfectly flat, deforms symmetrical about their neutral axis, has perfect mechanical constants (i.e. Young's Modulus, Poison's Ratio), and its deflections are small enough to allow the use of the Euler-Bernoulli beam theorem.

[1] A detailed derivation of Miller's method is shown in section 3, model and methods, of this thesis.

- The fluid is incompressible and isothermal, and the flow is steady and uniform for all flow channels at any given point along the channel length.

- Shear in the plates is considered negligible, and the plane stress assumption is applied.

- The plate edge supports are perfectly rigid.

Note that Miller's use of the beam equation and the wide beam approximation, are only an estimation of the effects observed. This is because the fuel plates in question are inherently plates, and not beams. The use of the wide beam approximation also assumes that there is no lateral deformation in the *z*-direction as shown in Figure 2-1, which implies that $\varepsilon_z \approx 0$, and that a plane stress state exist such that $\varepsilon_y \approx 0$ [28].

Figure 2-1 presents a general cantilever beam undergoing a load *P*, where the depth of the beam (*d*) is greater than the thickness (*t*) ($d \gg t$) which indicates a wide beam.

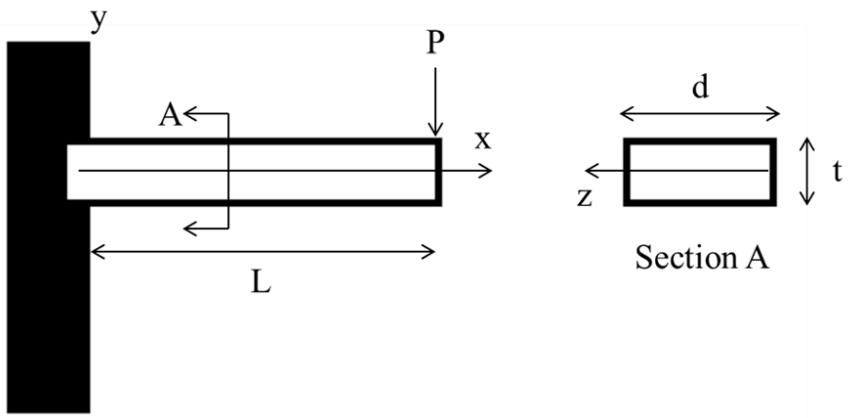

Figure 2-1: Basic cantilever, illustrating the wide beam approximation

The appropriateness of the application of the wide beam approximation may be debated. In most instances the deformation along the depth (z) of an actual fuel plate are in fact negligible. Also, the plane stress assumption remains valid along the depth. However, this is not true at the upstream or downstream edge of the plates (i.e. $z_{\max}$ and $z_{\min}$) [12],[15]. It is known that the plane stress state is not valid at the edges [29], and normal stress at the leading edge of the plate due to flow impingement causes a localized z-direction deformation. Regardless, most reactor fuel plates conform closely to the wide beam approximation because of their aspect ratios (i.e. $d >> t$).

Following Miller's study Zabriskie conducted experimental work to attempt to validate Miller's critical flow velocity [16],[30]. Zabriskie's experimental work addressed both measurements of critical flow velocity and the effects of varying length[2] and width[3] on critical flow velocity. He tested a number of assemblies with single plates, multiple plates, different channel dimensions, different lengths, and different widths. Most notably Zabriskie noted that the critical flow velocity predicted by Miller's method does not cause a collapse of the flow channel, rather a point of maximum plate deflection is reached. He also noted the effects at the leading edges (i.e. assembly inlet) were very pronounced, and could be easily mitigated with the addition of an "inlet support comb"[4]. One of the most ubiquitous trends started by Zabriskie was in comparing the measured critical velocity as a ratio to that predicted by Miller's method. Subsequent authors have continued this trend by not only using the ratio of measured critical flow velocities to Miller's method, but also the ratio of their own critical flow velocity models to Miller's method.

---

[2] Referred to as depth above, indicated by *d* in Figure 2-1.

[3] Represented by *L* in Figure 2-1

[4] An inlet support comb, restrains the leading edge of the fuel plates.

Kane advanced the area of hydro-mechanics following Zabriskie by preforming a theoretical analysis that varied the inlet spacing conditions [31]. He concluded that small deviation in the inlet spacing conditions, could have profound effects on the observed deflections

In 1963 Groninger and Kane tested three parallel plate assemblies [20]. Their work is of significant relevance to this study because some of the plates that were tested were of heterogeneous construction. Groninger and Kane worked around this construction by empirically testing these plates in a manner that allowed them to create a hypothetical equivalent plate of homogenous zirconium with an equivalent thickness. This hypothetical plate with equivalent thickness was then applied to Miller's method for predicting the critical flow velocity. The validity of such a method is difficult to gauge, because no details concerning the empirical test were provided by Groninger and Kane. The study presented had a number of interesting results which showed that the plates they tested never violently collapsed, but did show large deflections (as confirmed by Zabriskie [16]). The point of maximum deflection was measured at approximately twelve to fifteen inches from the inlet, for a plate with a total length of approximately eighty six inches. They also noted that the onset of plate vibration occurred at approximately 1.9 times Miller's critical flow velocity. Finally, they noted that adjacent plates consistently deform in opposite directions, with similar magnitudes.

Several authors have proposed modifications to Miller's work; this has typically taken the form of a variety of multiplicative coefficients. Johansen was the first to do this, and included a number of terms that quantify flow redistribution and frictional effects within the flow channel adjacent to the plate of interest [14]. Wambsganss did this as well; he attempted to capture some of the information "lost in the linearization process" by approximating the deformation contour in the span-width direction [13].

Of these modifications the work of Smith, has been employed in the nuclear safety culture more than others [12]. Smith chose to redefine critical flow velocity as critical dynamic pressure. Smith's model is also a semi-empirical model, based on a series of test preformed with gaseous fluid flows and several homogenous plate materials. He modified the theoretical analysis by including factors that quantified the increased deflection at the edges, and the angle of attack produced at the edge. These were termed the "area modification" and the "lift modification".

In 1968 Smissaert did experimental and analytical work in flow induced deflections and vibrations of flat plates [32]. Smissaert tested several sets of flat plates; most notably he performed tests with flow rates as high as three and a half times Miller's critical flow velocity. He experimentally observed two critical flow velocities, the first being the critical flow velocity predicted by Miller which signified the onset of large static deflections. The second was termed "flutter velocity" and signified the onset of plate vibrations. This was observed at approximately two times Miller's critical velocity.

Kim and Scarton used various computational tools to better analyze flow induced deflections near the inlet of an assembly [33]. They concluded that "viscous shear" played a large role in causing deflections at the plate's leading edge. They also confirmed earlier work that recommended the use of plates with very small aspect ratios.

More recently, in 2007, a series of tests were performed by Ho, Hong, and Mack in support of the Australian Replacement Research Reactor [34]. They observed that max deflection occurred at 75% of Millers critical flow velocity. It is important to note that their tests were performed without the use on an inlet support comb. This is significant because most authors have noted general agreement with the Miller's critical flow velocity only when a support comb was used.

2.2 Sandwich Structure Theory

The mechanics of laminated structures have been studied by many researchers. A subclass of laminated structures is that of sandwich structures; sandwich structures have three discrete layers (i.e. two outer layers and one inner layer). Sandwich structures became the subject of intense study due to efforts to lighten aircraft structures without compromising the rigidity of the structure [22],[23],[25],[35].

A very early study of sandwich structures was conducted by Gough, Elam, and DeBruyne in 1939 [36]. In it they discussed in detail a number of laminated structures and physical arguments as to why certain structural configurations are superior to others. This study contributed significantly to the body of knowledge in mechanics of laminate structures because it is explicit in stating the assumptions and reasoning behind sandwich structure design. They also, preformed a number of experiments and presented results for early laminates used in aircraft production.

Another early study of sandwich construction was conducted in 1941 by William et al. for the United Kingdom's Ministry of Aircraft Production [37]. This report is of note because it points out many distinctions between sandwich type construction, and other laminated constructions that may take a similar form. The primary difference between such structures centers on buckling of the sandwich plate; buckling is irreversible for plates with sandwich construction. This is because the inner and outer regions of a sandwich structure are bonded and move as one mechanical unit[5]. In addition William et al. presents an analytical and approximate theoretical solution for buckling of a sandwich plate that is simply supported on all four sides.

In 1948 Libove and Batdorf developed a form of 'small deflection theory' for sandwich plates [38], this work was performed under the National Advisory

[5] This is contrasted to "sheet stringer" construction, in which the buckling of any one component of the laminate may be reversible.

Committee for Aeronautics (NACA) an agency that later became known as the National Aeronautics and Space Administration (NASA). They developed both the energy expression and differential equation for displacement, for orthotropic[6] and isotropic plates.

Also in 1948, Reissner preformed a study that focused on effects on the core material (i.e. inner region material) [39]. He also developed quantitative methods for determining when solid mechanical analysis of a sandwich plate may no longer be analyzed linearly (i.e. small deflections), and noted that this effect becomes more pronounced as the core material became "softer".

Hoff and Mautner presented results for beams of sandwich construction [40]. Their solutions are relatively simple, and they presented experimental work that closely matched their theoretical values.

An important study, which has been cited by many authors to follow, was done by Hoff in 1950 for NACA [41]. Hoff solved the differential equation for bending, and buckling under compressive end loads for a sandwich plate with simply supported edge conditions.

Next Eringen presented the solution for a sandwich structure in which the face thicknesses were no longer considered to be thin, and "flattening" of the core material was taken into account [42]. This is important because it acknowledges cases in which the plane stress assumption is no longer valid.

In 1958 Ericksen preformed an analysis on sandwich structures that had unequal face material (i.e. outer region) thicknesses [43]. A number of simplifications that greatly aid in the analysis of sandwich structures with equal face thicknesses no longer apply

[6] An orthotropic material is one that has different mechanical properties in at least two of three mutually perpendicular directions. A classic example of this type of material is wood.

in the case where the faces are of unequal thickness. This results in a much more complex theoretical formulation for characterizing buckling of laminate plate structures.

A more recent paper by Yan and Dowell focused on vibrations in a sandwich structures, and cases in which the governing equations of motion may be acquired without directly solving the classical equations [44]. These cases are typically specialized and involve creating an equivalent beam with varying thickness, and may be thought of as a homogenization technique. Several other authors propose using techniques such as homogenization or the parallel axis theorem in order to find the flexural rigidity of a beam [22],[35],[45]. It is important to note that these methods are only valid in certain circumstances.

Much of the work in sandwich structures that was done in the latter part of the twentieth century has been collected into printed books on the subject. Three such books of note are by Vinson [23], Carlsson and Kardomateas [22], and Reddy [25]. The works of Vinson and Carlsson and Kardomateas proved especially useful in the writing of this thesis.

Vinson provides a significant amount of information on sandwich construction. This includes derivation of the governing equation, solutions for beams, columns, and rods, the application of energy methods to sandwich structures, the solutions for rectangular plates, dynamic effects and vibrations, and sandwich shells [23].

Carlsson and Kardomateas' work provides similar information as Vinson's. They include information on the derivation of the governing equations, first and higher order methods, global buckling, wrinkling and other localized instabilities, and information concerning de-bonding of layers [22].

2.3 Closing

The works presented in this chapter represent a significant amount of research effort in the fields of hydro-mechanical instabilities and laminate structural analysis. While a number of works have analyzed hydro-mechanical instabilities of homogenous plates, very few have theoretically focused on plates of laminated construction. As noted this study aims to incorporate laminate structural analysis into the study of hydro-dynamical instability.

A number of additional references were used in this study, and have been cited within the bibliography. Table 2-1 provides a summary of the literature reviewed organized by subject and study technique (i.e. experimental or theoretical).

Table 2-1: Summary of literature surveyed

Authors	Subject of Investigation			
	Flow Induced Deflections		Sandwich Structure	
	Experimental Work	Theoretical Work	Experimental Work	Theoretical Work
Stromquist, W.K. & Sisman, O [26]	X			
Doan, R.L. [27]	X			
Miller, D.R. [11]		X		
Zabriskie, W.L. [16][30]	X			
Kane, J.J. [31]		X		
Groninger, R.D. & Kane, J.J. [20]	X			
Wambsganss, M.W. [13]		X		
Johansson, R.B. [14]		X		
Smith, R.L. [12]	X	X		
Smissaert, G.E. [32]	X	X		
Kim, Y.T. & Scarton, H.A. [33]		X		
Ho, M., Guang Hong, & Mack, A.N.F. [34]	X			
Gough, G.S., Elam, C.F., & DeBruyne, N.A.[36]			X	X
Williams, D., Leggett, D.M.A. & Hopkins, H.G. [37]			X	X
Libove, C. & Batdorf, S.B. [38]				X
Reissner, E. [39]				X
Hoff, N.J. & Mautner, S.E. [40]			X	X
Hoff, N.J. [41]				X
Eringen, A.C. [42]				X
Ericksen, W.S. [43]				X
Yan, M.J. & Dowell, E.H. [44]				X
Carlsson, L.A. & Kardomateas, G.A. [22]			X	X
Vinson, J.R. [23]			X	X
Reddy, J.N [25]			X	X

3 MODEL AND METHODOLOGY

This chapter describes the derivation and physical construct of two unique models used to estimate the critical flow velocity and critical dynamic pressure difference necessary to cause plate collapse for a laminate plate having three discrete regions. These models follow a formal two step methodology. The first step defines the hydraulic domain which results in the net force on the plate of interest as a function of the plate's flexural rigidity. The second step focuses exclusively on flexural rigidity, and the different perspectives one may take when constructing this term.

3.1 Critical Flow Velocity and Critical Dynamic Pressure

The critical flow velocity that predicts plate collapse for a flat rectangular plate was first formally derived by D.R. Miller [11]. Since then numerous studies have been performed on the subject of critical flow velocity, many of which propose new and innovative methods to quantify and explain this phenomena. All known studies which focus on Miller's original method have only dealt with homogenous plates, as such these studies and subsequent models have incorporated the material and geometric properties of a homogenous plate. While the following derivation shares many similarities to Miller's original work, it also expands on it and all known previous studies by creating three discrete mathematical regions for a rectangular flat laminate plate while maintaining continuity of stress throughout each cross-sectional region.

In order to determine the critical flow velocity for a laminated plate, a relation must be first formulated in terms of flexural rigidity. This is done through a simple modification to the Euler-Bernoulli beam equation [17],[46]. This modification takes place through the grouping of all material properties, and geometric information for a given cross-sectional region within the flexural rigidity (D) term.

$$D\frac{d^4y}{dx^4} = P(x) \tag{3.1}$$

Equation (3.1) represents the out of plane deflection (y) in relation to the imposed pressure on the beam (P) as a function of span width (x), and flexural rigidity (D). This study's motivation centers on reactor fuel plates, as such there are three beam boundary conditions which are commonly used for reactor safety analysis. These three boundary conditions refer to the edges of the plate, including: (a) clamped on both edges, (b) clamped on one edge and simply supported on the other, and (c) simply supported on both edges [47]. These are shown in Figure 3-1 below. The following outlines the complete derivation assuming both edges of the plate are clamped. For thoroughness, the derivation for the case regarding plates having a clamped edge and simply supported edge, and plates have both edges simply supported may be found in Appendix A.

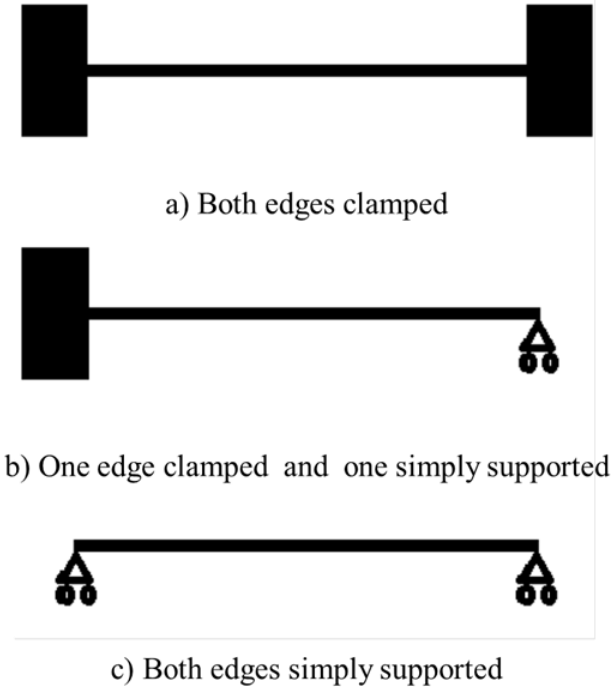

Figure 3-1: Three edge boundary conditions considered

The general plate arrangement and unperturbed flow channel geometry are shown in Figure 3-2, where (h) is the channel height and (L) is the span width.

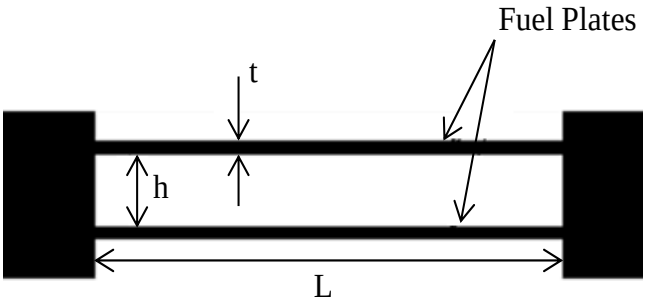

Figure 3-2: Plate and flow channel geometry

Solving equation (3.1), assuming both edges clamped yields the following analytical equation for out of plane deflection [17].

$$y(x) = \frac{P}{24D}\left(x^4 - 2Lx^3 + L^2x^2\right) \tag{3.2}$$

It is assumed in this study that the fluid flow, or hydraulic load imposed on the plate(s), is steady at an instant in time the plate(s) begin to deform resulting in a change in flow area. This change is found by doubling the integration of equation (3.2) across the entire span width of a plate ($x: 0 \rightarrow L$). The change in flow area impacts the hydraulic domain by yielding a net pressure between adjacent channels. The net pressure is also the boundary condition imposed on the solid domain (i.e. the plate), which results in out of plain deflection. Assuming that the original cross-sectional area is of perfect rectangular geometry, the original flow channel may be represented as the product of channel height (h) and span width (L) yielding $A_0 = Lh$. The relative change in flow area may then be quantified by dividing the perturbed area found by integrating the beam deflection equation, by the original flow channel area as seen in (3.3).

$$\frac{\Delta A}{A_o} = \frac{PL^4}{360Dh} \tag{3.3}$$

Equation (3.3) provides a relation between an imposed pressure (*P*) on a set of beams, relative the beam's change in out of plane position.

Now that the solid mechanics of the problem has been defined, it is necessary to identify an equation that describes the fluid mechanics of the problem which relates those forces imposed by the fluid to the change in deflection of the plate under. This is done through simplification of the conservation of energy, into Bernoulli's equation.

$$\frac{\delta Q}{\partial t}-\frac{\delta W}{\partial t}=\frac{\partial}{\partial t}\iiint_{\text{c.v.}}\vartheta\rho dV+\iint_{\text{c.s.}}\left(\vartheta+\frac{P}{\rho}\right)\rho\left(\bar{\text{v}}\cdot\bar{\text{n}}\right)dS \tag{3.4}$$

The simplification begins by noting that $\vartheta=\varsigma+\bar{u}^2/2+gz$ is the specific energy which includes the internal energy (ς), the kinetic energy ($\bar{u}^2/2$), and the potential energy (*gz*)[48][49]. Integrating equation (3.4) assuming that the flow is steady, no work is done, no heat is produced, and the cross sectional flow area is constant along the length, yields what is known as Bernoulli's equation.

$$\left(\frac{P}{\rho}+\frac{v^2}{2}+gz\right)_2-\left(\frac{P}{\rho}+\frac{v^2}{2}+gz\right)_1=0 \tag{3.5}$$

The *P* term is pressure, ρ is fluid density, *v* is fluid velocity, *g* is the acceleration of gravity, and *z* is the height.

It may be assumed that the gravitational terms are insignificant; equation (3.5) can be reformulated into the following. This represents the net pressure difference between two channels.

$$P_1-P_2=\Delta P=\frac{1}{2}\rho\left(v_2^2-v_1^2\right) \tag{3.6}$$

In order to use equation (3.6), relations for each velocity term (v) must developed. This is done by applying the conservation of mass, through a control volume shown by equation (3.7).

$$\frac{\partial}{\partial t}\int_{CV}\rho dV + \int_{CS}\rho(v\cdot\bar{n})\,dA = 0 \tag{3.7}$$

The volume integral represents the accumulation of mass in a control volume with respect to time, and the surface integral is taken to be the difference between the mass exiting the control volume to mass entering the control volume. Equation (3.7) is commonly referred to as the continuity equation, which is simply the conservation of mass on a control volume [48],[49].

Using greens theorem, the surface integral in equation (3.7) can be converted to a volume integral shown in (3.8).

$$\int_{CS}\rho(v\cdot\bar{n})\,dA \rightarrow \int_{CV}\nabla\cdot\rho v dV \tag{3.8}$$

Assuming steady flow of an incompressible fluid, equation (3.7) may be simplified. The steady flow assumption causes the time dependent terms to go to zero, and the incompressible assumption infers that there is no change in fluid density (ρ). The simplification is as follows.

$$\nabla\cdot v = 0 \tag{3.9}$$

Integration of equation (3.9), for a one dimensional control volume assuming steady flow and an incompressible fluid yields the following.

$$A_i v_i = A_j v_j \tag{3.10}$$

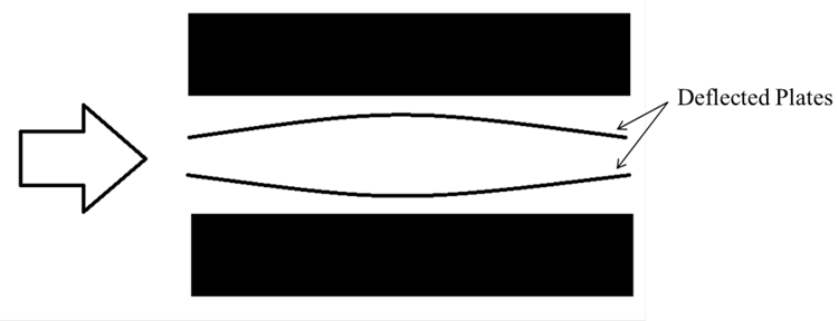

Figure 3-3: Sectional view of flow channel, and deflected plates

The changes in flow area for two adjacent flow channels are now applied; this change is illustrated in Figure 3-3. It is assumed that two adjacent plates will deflect in opposite directions. Assuming the top plate was deflected upwards then the bottom plate would deflect downward with equal magnitude. This observation has been verified both theoretically and empirically [11],[20].

When it is assumed that each plate deflects in opposite direction, with equal magnitude, the increase in one flow channel is given by equation (3.11).

$$\left(A_o + \Delta A\right) v_1 = A_o v_o \tag{3.11}$$

While the decrease in the neighboring flow channel is given by (3.12).

$$\left(A_o - \Delta A\right) v_2 = A_o v_o \tag{3.12}$$

The term v_0 is the initial flow velocity in the respective channel, and v_1 and v_2 are channel 1 and 2 velocities after a flow area perturbation of $\Delta A\left(A_0\right)^{-1}$. Note that from equations (3.11) and (3.12) it is assumed that the initial velocities (v_0) of channel 1 and 2 are assumed to be equal. Reformulating equations (3.11) and (3.12) in respect

to their initial velocities after a given change in flow area yields equation (3.13) for channel 1 and equation (3.14) for channel 2.

$$v_1 = \frac{v_o}{1+\Delta A\left(A_o\right)^{-1}} \tag{3.13}$$

$$v_2 = \frac{v_0}{1-\Delta A\left(A_o\right)^{-1}} \tag{3.14}$$

The net pressure may now be linearized by equating (3.6), (3.13), and (3.14) while taking the Taylor expansion as $\Delta A\left(A_0\right)^{-1}$ goes to zero. The linearized pressure is a key assumption in formulating critical flow velocity and critical dynamic pressure. The linearization yields.

$$\Delta P = 2\rho v_o^2 \Delta A\left(A_o\right)^{-1} \tag{3.15}$$

Equations (3.3) and (3.15) are now combined, resulting in the critical flow velocity for a flat plate having both edge boundaries conditions clamped given by equation (3.16).

$$V_{cr} = \left(\frac{h}{\rho L^4}\right)^{1/2} \left(180D\right)^{1/2} \tag{3.16}$$

The critical flow velocity for a plate having one edge boundary condition clamped and the other simply supported is given by (3.17).

$$V_{cr} = \left(\frac{h}{\rho L^4}\right)^{1/2} \left(80D\right)^{1/2} \tag{3.17}$$

The critical flow velocity for a plate having both edge boundary conditions simply supported is given by (3.18).

$$V_{cr} = \left(\frac{h}{\rho L^4} \right)^{1/2} \left(30D \right)^{1/2} \tag{3.18}$$

As mentioned, a comprehensive derivation of equations (3.17), and (3.18) is presented in appendix A.

Equations (3.16), (3.17), and (3.18) represent the most fundamental forms of critical flow velocity for a single flat plate for each of the three edge boundary conditions analyzed in this study. This form is left in terms of flexural rigidity (D), which will be discussed in subsequent sections of this chapter. It is useful to group the critical flow velocity terms such that all hydraulic components including channel height (h), channel span width (L), and fluid density (ρ) together while solid mechanical components such as flexural rigidity (D) are grouped separately.

Note that in (3.16), (3.17), and (3.18) the coefficient tied to the flexural rigidity term is the only component of the equation that changes as the edge boundary condition changes. This demonstrates, that the critical flow velocity required for a plate with both edges clamped as seen in (3.16) is much larger in magnitude from that of a plate having both edges simply supported (3.18). This is expected, and agrees with basic solid mechanical [17].

An alternate formulation for the critical flow velocity (v_{cr}) is of the form defined by critical dynamic pressure where dynamic pressure (q) is shown to be.

$$q = \frac{1}{2} \rho v^2 \tag{3.19}$$

Smith was the first to demonstrate the usefulness, of quantifying plate collapse in terms of critical dynamic pressure [12]. This is done by equating the velocity in (3.19) to the critical flow velocity. Equations (3.16), (3.17), and (3.18) may be reformulated in this fashion.

The critical dynamic pressure for a plate with both edges clamped is given by (3.20).

$$q_{cr} = \left(\frac{h}{L^4}\right)(180D) \tag{3.20}$$

For a plate with one edge clamped and the other simply supported is given by (3.21).

$$q_{cr} = \left(\frac{h}{L^4}\right)(80D) \tag{3.21}$$

For a plate with both edges simply supported is given by .

$$q_{cr} = \left(\frac{h}{L^4}\right)(30D) \tag{3.22}$$

3.2 Flexural Rigidity

If left as currently defined, equations (3.16), (3.17), and (3.18) may be solved given a homogenous flat plate by applying the flexural rigidity shown in equation (3.23), yielding critical flow velocity as defined by Miller in 1958 [11].

$$D = \frac{t^3}{12}\frac{E}{\left(1-\nu^2\right)} \tag{3.23}$$

The work described herein extends Miller's method for predicting critical flow velocity, by quantifying this phenomenon for a heterogeneous lamented plate having

three discrete layers. This is done, by formulating flexural rigidity for a laminated plate.

The flexural rigidity contains all of the information pertaining to material properties and geometry, for a given cross-section. The flexural rigidity may be thought of as "stiffness". Stiffness is simply a cross-sections resistance to deflection, as seen in (3.23).

A case where a plate has three discrete regions, with both outer regions having equal thickness and being symmetric about the centerline is known as a sandwich structure [22][23]. Sandwich structures are a subclass of structures studied in composites. The motivation for developing a critical flow velocity relation, which incorporates the characteristics of a sandwich structure, is driven by the desire to analyze reactor fuel plates. Reactor fuel plates, comprised of three discrete layers typically have two outer cladding regions and one inner fueled region. The outer two layers of the LEU fuel introduced in this study are made of Aluminum while the inner region is comprised of Uranium-Molybdenum alloy.

Previous authors have done significant work in analyzing the mechanics of sandwich structures [22],[23],[25]. The aim of this work is to adapt and extend previous work in a manner that is useful to studying the mechanics of reactor fuels, with a hydraulic boundary.

Prior to defining and expanding on flexural rigidity, it is important to note that although a traditional reactor fuel plate is clad all around with an outer layer, it is assumed during this study that this outer layer is defined only on the top and bottom of the inner region; this is shown in Figure 3-4.

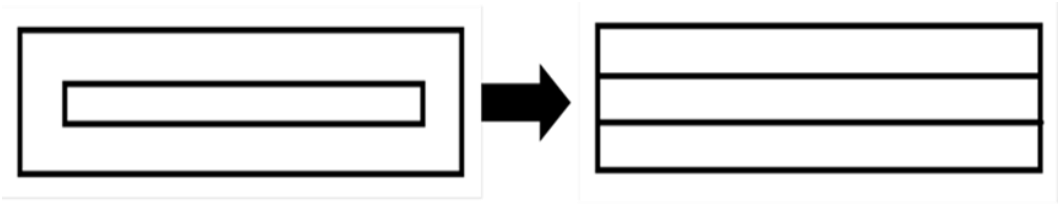

Figure 3-4: Plate geometry simplification

The actual fuel plate is shown on the left in Figure 3-4, while the simplified geometry is shown on the right. This geometric simplification is made in order to better characterize each discrete region's flexural rigidity. This simplification does not significantly impact the solution, based on the fact that flexural rigidity is highly dependent on thickness rather than width. This is true for all beams having a large length to thickness ratios, and is shown mathematically by the second area moment of inertia for a cross-section in which the thickness term is raised to the third power. Thus variations across the width of a sandwich structure are of little importance, while variations across the thickness are highly important.

Furthermore, it is common practice to analyze flexural rigidity in terms of unit width[7] [50], as is done throughout this study.

The dependence of stiffness on thickness indicates that the outermost fiber of a beam contributes the most to the flexural rigidity, and the overall stiffness. This is the fundamental driving force behind the structural mechanics of sandwich structure design. The sandwich's outermost layers are considered to contribute greatly to the stiffness of the structure, while the inner region contributes much less.

An implication of the sandwich structure model is that no slip may occur at the interface of each layer. If such slip occurs the structure is no longer a sandwich structure and cannot be analyzed using such techniques.

[7] Some early references refer to flexural rigidity in terms of unit width as 'specific flexural rigidity'.

Figure 3-5 shows the general sandwich structure analyzed throughout this study. The body in Figure 3-5 is symmetric about the centerline of the plate, and each region is isotropic and homogenous.

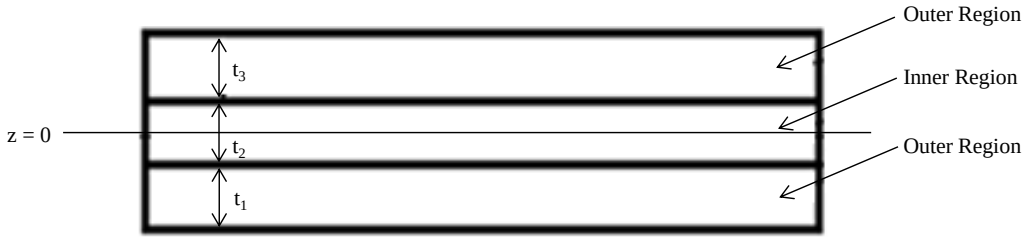

Figure 3-5: General sandwich structure analyzed in this study

3.2.1 The Monocoque Analogy

A monocoque is a structure that is supported by its skin [23]. The sandwich structure presented in Figure 3-5 may be thought of as a monocoque, because the outer region contributes the most to flexural rigidity. The flexural rigidity of a sandwich structure may be approximated, by assuming the outer region of the sandwich structure bares the entire load on the plate. This section derives and defines a version of flexural rigidity, based on this and terms it the monocoque analogy. Note that the monocoque analogy is a simplified estimation of a plate's flexural rigidity, as all loading is assumed to be taken by the outer regions (regions 1 and 3 in Figure 3-5), because of this the applicability of this method will be discussed later.

The flexural rigidity for a sandwich structure using the monocoque analogy is shown below in equation (3.24).

$$D_{mon} = \frac{\left(t_{IR} + t_{OR}\right)^2 t_{OR}}{2} \frac{E_{OR}}{\left(1 - \nu_{OR}^2\right)} \tag{3.24}$$

Equation (3.24), was first derived by Carlson and Kardomateas [22]. Carlson and Kardomateas derived this relation for the application to structures used in the aerospace industry. It is important to note that Carlson and Kardomateas defined each region at its centroid in reference to the sandwich centerline. This is in contrast to other work, which defined each region at its interface [23].

In order to arrive at the monocoque analogy form of flexural rigidity the general stress states must be simplified into a one dimensional form. This form is necessary because the critical flow velocity and critical dynamic pressure functions have been developed assuming a one-dimensional flexural rigidity.

Figure 3-6 is a general body referring to the general stress state presented in equation (3.25), assuming a Cartesian coordinate system.

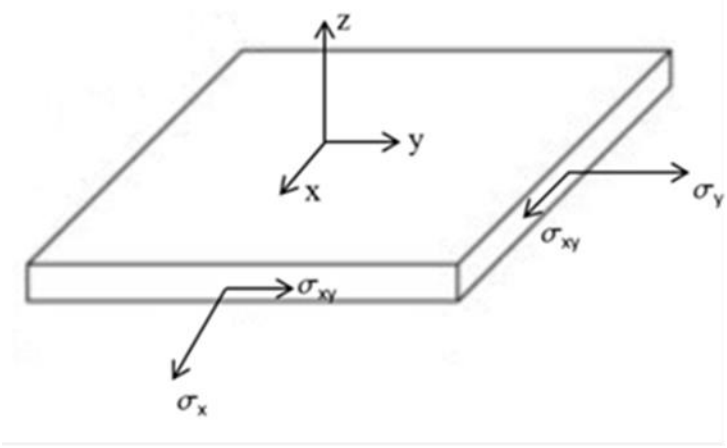

Figure 3-6: Flat plate coordinate system, showing stress directions

Applying Hooke's Law to the body in Figure 3-6, yields the general stress state for the *k*-th region of a sandwich structure shown by equation (3.25). The six by six coefficient matrix is most commonly referred to as the stiffness matrix having discrete stiffness parameters $\overline{Q_{ij}}$.

$$\begin{bmatrix} \sigma_x \\ \sigma_y \\ \sigma_z \\ \sigma_{yz} \\ \sigma_{xz} \\ \sigma_{xy} \end{bmatrix}_k = \begin{bmatrix} \overline{Q_{11}} & \overline{Q_{12}} & \overline{Q_{13}} & \overline{Q_{14}} & \overline{Q_{15}} & \overline{Q_{16}} \\ \overline{Q_{21}} & \overline{Q_{22}} & \overline{Q_{23}} & \overline{Q_{24}} & \overline{Q_{25}} & \overline{Q_{26}} \\ \overline{Q_{31}} & \overline{Q_{32}} & \overline{Q_{33}} & \overline{Q_{34}} & \overline{Q_{35}} & \overline{Q_{36}} \\ \overline{Q_{41}} & \overline{Q_{42}} & \overline{Q_{43}} & \overline{Q_{44}} & \overline{Q_{45}} & \overline{Q_{46}} \\ \overline{Q_{51}} & \overline{Q_{52}} & \overline{Q_{53}} & \overline{Q_{54}} & \overline{Q_{55}} & \overline{Q_{56}} \\ \overline{Q_{66}} & \overline{Q_{62}} & \overline{Q_{63}} & \overline{Q_{64}} & \overline{Q_{65}} & \overline{Q_{66}} \end{bmatrix}_k \begin{bmatrix} \varepsilon_x \\ \varepsilon_y \\ \varepsilon_z \\ 2\varepsilon_{yz} \\ 2\varepsilon_{xz} \\ 2\varepsilon_{xy} \end{bmatrix}_k \tag{3.25}$$

Equation (3.25) may be simplified by assuming that each layer is isotropic in material and stress load characteristics. In the application to reactor fuel plates this assumption is valid, because the Aluminum outer regions and Uranium-Molybdenum inner regions are isotropic [24],[51]. The isotropic assumption reduces equation (3.25) to equation (3.26).

$$\begin{bmatrix} \sigma_x \\ \sigma_y \\ \sigma_z \\ \sigma_{yz} \\ \sigma_{xz} \\ \sigma_{xy} \end{bmatrix}_k = \begin{bmatrix} \overline{Q_{11}} & \overline{Q_{12}} & \overline{Q_{12}} & 0 & 0 & 0 \\ \overline{Q_{12}} & \overline{Q_{11}} & \overline{Q_{12}} & 0 & 0 & 0 \\ \overline{Q_{12}} & \overline{Q_{12}} & \overline{Q_{11}} & 0 & 0 & 0 \\ 0 & 0 & 0 & \overline{Q_{66}} & 0 & 0 \\ 0 & 0 & 0 & 0 & \overline{Q_{66}} & 0 \\ 0 & 0 & 0 & 0 & 0 & \overline{Q_{66}} \end{bmatrix}_k \begin{bmatrix} \varepsilon_x \\ \varepsilon_y \\ \varepsilon_z \\ 2\varepsilon_{yz} \\ 2\varepsilon_{xz} \\ 2\varepsilon_{xy} \end{bmatrix}_k \tag{3.26}$$

Note that the stiffness matrix is diagonally symmetric due to the homogeneity of material composition and comprises three of the original thirty six stiffness parameters. Equation (3.26) may be further simplified assuming a plane stress state.

A plane stress state exists when $\sigma_z = \sigma_{yz} = \sigma_{xz} = 0$, which states that the out of plane normal stress and out of plane shear terms are zero. To implement this assumption one must start with the strain of an isotropic body shown in equation (3.27), and input $\sigma_z = \sigma_{yz} = \sigma_{xz} = 0$ into the solution matrix. The coefficient matrix shown in equation (3.27) is commonly referred to as the compliance matrix.

$$\begin{bmatrix} \varepsilon_x \\ \varepsilon_y \\ \varepsilon_z \\ 2\varepsilon_{yz} \\ 2\varepsilon_{xz} \\ 2\varepsilon_{xy} \end{bmatrix}_k = \frac{1}{E_k} \begin{bmatrix} 1 & -\nu & -\nu & 0 & 0 & 0 \\ -\nu & 1 & -\nu & 0 & 0 & 0 \\ -\nu & -\nu & 1 & 0 & 0 & 0 \\ 0 & 0 & 0 & 2(1+\nu) & 0 & 0 \\ 0 & 0 & 0 & 0 & 2(1+\nu) & 0 \\ 0 & 0 & 0 & 0 & 0 & 2(1+\nu) \end{bmatrix}_k \begin{bmatrix} \sigma_x \\ \sigma_y \\ 0 \\ 0 \\ 0 \\ \sigma_{xy} \end{bmatrix}_k \tag{3.27}$$

In equation (3.27); ν represents Poisons Ratio for the *k*-th layer and *E* represents Young's Modulus for the *k*-th layer. The compliance matrix is reduced as shown in equation (3.28). This is simply the plane strain matrix.

$$\begin{bmatrix} \varepsilon_x \\ \varepsilon_y \\ 2\varepsilon_{xy} \end{bmatrix}_k = \frac{1}{E_k} \begin{bmatrix} 1 & -\nu & 0 \\ -\nu & 1 & 0 \\ 0 & 0 & 2(1+\nu) \end{bmatrix}_k \begin{bmatrix} \sigma_x \\ \sigma_y \\ \sigma_{xy} \end{bmatrix}_k \tag{3.28}$$

Equation (3.28) must now be inverted in order to transform the compliance matrix (strain) into the stiffness matrix (stress).

$$\begin{bmatrix} \sigma_x \\ \sigma_y \\ \sigma_{xy} \end{bmatrix}_k = \frac{E_k}{(1-\nu_k^2)} \begin{bmatrix} 1 & \nu & 0 \\ \nu & 1 & 0 \\ 0 & 0 & \frac{1}{2}(1-\nu) \end{bmatrix}_k \begin{bmatrix} \varepsilon_x \\ \varepsilon_y \\ 2\varepsilon_{xy} \end{bmatrix}_k \tag{3.29}$$

Equation (3.29) is the plane stress matrix for the *k*-th layer of a sandwich structure.

For direct integration into the critical flow velocity or critical dynamic pressure the one dimensional plane stress case must be taken. This further simplifies the relation yielding the plane stress for the *k*-th layer of the sandwich structure.

$$\sigma_k = Q_k \varepsilon_k = \frac{E_k}{\left(1-\nu_k^2\right)} \varepsilon_k \tag{3.30}$$

Equation (3.30) can be re-written for the bottom layer of the sandwich and the top layer of the sandwich shown as (3.31) and (3.32), respectively.

$$\sigma_1 = \frac{E_1}{\left(1-\nu_1^2\right)} \varepsilon_1 \tag{3.31}$$

$$\sigma_3 = \frac{E_3}{\left(1-\nu_3^2\right)} \varepsilon_3 \tag{3.32}$$

The bending strain for each layer must now be considered. To do this it is useful to define the bending displacement of the sandwich structure in terms of its curvature. This is shown in equation (3.33) where $u_0(x)$ is the displacement of the inner region; *z* is term that defines the distance from the center of the sandwich, and κ is the curvature of the structure[8].

$$u(x) = u_0(x) + z\kappa \tag{3.33}$$

The derivative of displacement with respect to *x* is taken yielding the bending strain on the sandwich structure.

$$\varepsilon = \frac{\partial u_0}{\partial x} + z\kappa \tag{3.34}$$

Equation (3.34), may be reworked in the form of the inner region's strain. This is the bending strain on the sandwich structure, in terms of the *k*-th layer.

---

[8] A detailed explanation of this displacement function can be found on pgs. 53-57 of Carlsson and Kardomateas [22] and/or pgs. 44-47 of Vinson [23].

$$\varepsilon_k = \varepsilon_x^0 + z_k \kappa \tag{3.35}$$

The bending strain for the bottom region is shown in equation (3.36), and the top region is shown in equation (3.37). These relations are acquired by inputting the appropriate values of *z*, which is calculated from the centerline of the sandwich to the centroid of each layer.

$$\varepsilon_1 = \varepsilon_x^0 - \frac{(t_1 + t_2)}{2} \kappa \tag{3.36}$$

$$\varepsilon_3 = \varepsilon_x^0 + \frac{(t_2 + t_3)}{2} \kappa \tag{3.37}$$

The force resultant *N* and moment couple *M* for the *k*-th layer is generated by creating a force balance on the generic body shown in Figure 3-7.

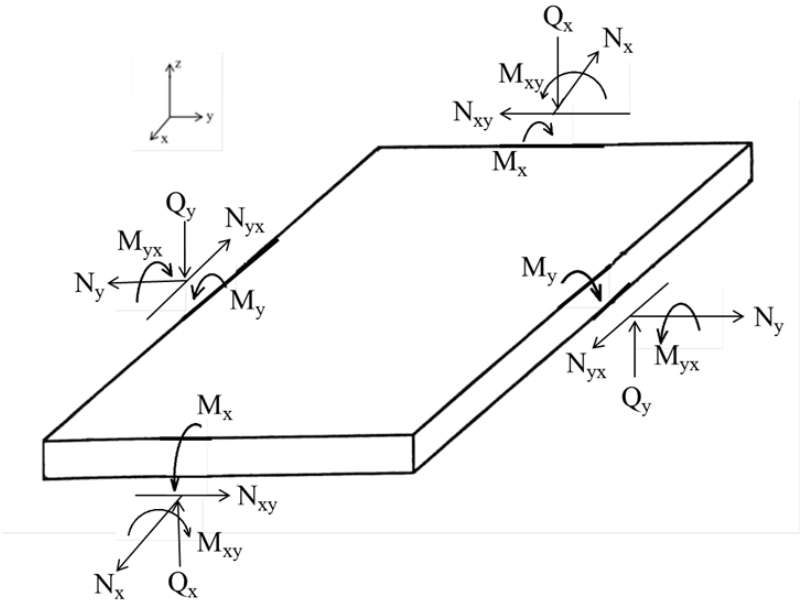

Figure 3-7: Force and moment balance on a generic plate

The force resultants are shown in equation (3.38) and each moment couple is presented in equation (3.39).

$$\begin{bmatrix} N_x \\ N_y \\ N_{xy} \end{bmatrix}_k = \int_{-\left(\frac{t_2}{2}+t_1\right)}^{-\frac{t_2}{2}} \begin{bmatrix} \sigma_x \\ \sigma_y \\ \sigma_{xy} \end{bmatrix} dz + \int_{\frac{t_2}{2}}^{\left(\frac{t_2}{2}+t_3\right)} \begin{bmatrix} \sigma_x \\ \sigma_y \\ \sigma_{xy} \end{bmatrix} dz \tag{3.38}$$

$$\begin{bmatrix} M_x \\ M_y \\ M_{xy} \end{bmatrix}_k = \int_{-\left(\frac{t_2}{2}+t_1\right)}^{-\frac{t_2}{2}} \begin{bmatrix} \sigma_x \\ \sigma_y \\ \sigma_{xy} \end{bmatrix} z dz + \int_{\frac{t_2}{2}}^{\left(\frac{t_2}{2}+t_3\right)} \begin{bmatrix} \sigma_x \\ \sigma_y \\ \sigma_{xy} \end{bmatrix} z dz \tag{3.39}$$

Note the limits of integration, are from the center line of the sandwich panel to the centroid of the *k*-th layer.

Equations (3.40) and (3.41) show the force resultant and moment couple of a one dimensional sandwich plate, with only the outer regions accounted for.

$$N_x = \int_{t_1-\frac{t_2}{2}}^{-\frac{t_2}{2}} \sigma_1 dz + \int_{\frac{t_2}{2}}^{\frac{t_2}{2}+t_3} \sigma_3 dz \tag{3.40}$$

$$M_x = \int_{t_1-\frac{t_2}{2}}^{-\frac{t_2}{2}} \sigma_1 z dz + \int_{\frac{t_2}{2}}^{\frac{t_2}{2}+t_3} \sigma_3 z dz \tag{3.41}$$

Substitution of the stress terms and integration of the force resultant and moment couple, yields equations (3.42) and (3.43). These are the general relations for the force resultants *N* and moment couples *M*, for an isotropic sandwich plate in a plane stress state. Where *A* is the extensional stiffness, *D* is the flexural rigidity, and *B* and *C* are elastic coefficients.

$$\begin{bmatrix} N_x \\ N_y \\ N_{xy} \end{bmatrix} = \begin{bmatrix} A_{11} & A_{12} & A_{16} \\ A_{12} & A_{22} & A_{26} \\ A_{16} & A_{26} & A_{66} \end{bmatrix} \begin{bmatrix} \varepsilon_x^0 \\ \varepsilon_y^0 \\ 2\varepsilon_{xy}^0 \end{bmatrix} + \begin{bmatrix} B_{11} & B_{12} & B_{16} \\ B_{12} & B_{22} & B_{26} \\ B_{16} & B_{26} & B_{66} \end{bmatrix} \begin{bmatrix} \kappa_x \\ \kappa_y \\ \kappa_{xy} \end{bmatrix} \tag{3.42}$$

$$\begin{bmatrix} M_x \\ M_y \\ M_{xy} \end{bmatrix} = \begin{bmatrix} C_{11} & C_{12} & C_{16} \\ C_{12} & C_{22} & C_{26} \\ C_{16} & C_{26} & C_{66} \end{bmatrix} \begin{bmatrix} \varepsilon_x^0 \\ \varepsilon_y^0 \\ 2\varepsilon_{xy}^0 \end{bmatrix} + \begin{bmatrix} D_{11} & D_{12} & D_{16} \\ D_{12} & D_{22} & D_{26} \\ D_{16} & D_{26} & D_{66} \end{bmatrix} \begin{bmatrix} \kappa_x \\ \kappa_y \\ \kappa_{xy} \end{bmatrix} \tag{3.43}$$

The one dimensional form of (3.42) and (3.43) is presented by equations (3.44) and (3.45).

$$N = A\varepsilon_x^0 + Bk \tag{3.44}$$

$$M = C\varepsilon_x^0 + Dk \tag{3.45}$$

It must now be stated that the sandwich plate in question is symmetric about the it's centerline. In this case, then $[B] = 0 = [C]$. It is also observed that the thicknesses of the outer regions are of equal thickness (i.e. $t_1 = t_3 = t_{OR}$). These assumptions allow for equations (3.42) and (3.43) as well as equations (3.44) and (3.45), to be uncoupled. This yields equations (3.46) and (3.47) for the general case.

$$\begin{bmatrix} N_x \\ N_y \\ N_{xy} \end{bmatrix} = \begin{bmatrix} A_{11} & A_{12} & A_{16} \\ A_{12} & A_{22} & A_{26} \\ A_{16} & A_{26} & A_{66} \end{bmatrix} \begin{bmatrix} \varepsilon_x^0 \\ \varepsilon_y^0 \\ 2\varepsilon_{xy}^0 \end{bmatrix} \tag{3.46}$$

$$\begin{bmatrix} M_x \\ M_y \\ M_{xy} \end{bmatrix} = \begin{bmatrix} D_{11} & D_{12} & D_{16} \\ D_{12} & D_{22} & D_{26} \\ D_{16} & D_{26} & D_{66} \end{bmatrix} \begin{bmatrix} \kappa_x \\ \kappa_y \\ \kappa_{xy} \end{bmatrix} \tag{3.47}$$

Equations (3.48) and (3.49) represent (3.46) and (3.47) in a one dimensional state.

$$N = A\varepsilon_x^0 \tag{3.48}$$

$$M = D\kappa_x \tag{3.49}$$

It may be seen by inspection that the form of the extensional stiffness matrix *A* in equation (3.42), and the stiffness parameter matrix *C* in equation (3.43), are nearly identical in form to the stiffness matrix *Q* in equation (3.29). In fact they only differ by a factor of *t*, that is $A=tQ$. Furthermore, the grouping of terms during the integration of equation (3.41), noting that the force resultant and moment couple are now independent, allows the bending stiffness matrix (i.e. flexural rigidity) *D* to be filled independently of κ. This yields a simple relation for the one-dimensional case[9] of *D*, shown in equation (3.50) where $A=tQ$.

$$D = \frac{1}{4}\left(\left(t_2 + t_1\right)^2 A_1 + \left(t_2 + t_3\right)^2 A_3\right) \tag{3.50}$$

From the assumption of symmetry and equal thickness for the outer region, it is assumed that extensional stiffness for each region is equal (i.e. $A_1 = A_3 = A_{OR}$). The subscript "OR" refers to the outer region of the sandwich plate. This implies that the extensional stiffness, for the sandwich structure, is the following.

$$A = A_1 + A_3 = 2A_{OR} \tag{3.51}$$

Combining equations (3.50) and (3.51) yields the following relation for flexural rigidity.

---

[9] Relations for the coefficient matrices *A* and *D* are independent of strain ε_x^0 and κ, allowing them to be found by grouping terms after integration. The reader will find this explained again in the "ideal laminate section" of this thesis, and is referred to there for further explanation.

$$D = \frac{\left(t_{IR} + t_{OR}\right)^2}{2} A_{OR} \tag{3.52}$$

Recall that the outer regions are of equal thickness, with equivalent material properties. This is restated below.

$$t_{OR} = t_1 = t_3 \tag{3.53}$$

$$E_{OR} = E_1 = E_3 \tag{3.54}$$

$$\nu_{OR} = \nu_1 = \nu_3 \tag{3.55}$$

The interior region of the sandwich structure (region 2 in Figure 3-5) will be denoted with the subscript "IR" indicating the inner region.

Combining and reformulating equation (3.51), yields the extensional stiffness for the monocoque analogy (3.56).

$$A_{mon} = \frac{2E_{OR}t_{OR}}{\left(1-\nu_{OR}^2\right)} \tag{3.56}$$

Inserting the extensional stiffness given by equation (3.56) into the previously defined flexural rigidity term seen in equation (3.52), yields the flexural rigidity for the monocoque analogy.

$$D_{mon} = \frac{\left(t_{IR} + t_{OR}\right)^2 t_{OR}}{2} \frac{E_{OR}}{\left(1-\nu_{OR}^2\right)} \tag{3.24}$$

Hereinafter results referring to the monocoque analogy will use the form presented in equation (3.24).

3.2.1.1 Synopsis and Applicability of the Monocoque Analogy

It is commonly known that the outermost fiber in a beam contributes the most to stiffness of the beam as theoretically and experimentally demonstrated through numerous studies [17],[19],[28],[46]. Sandwich structures take advantage of this by moving material away from the inner region. Historically, this has been done to lighten structures while maintaining mechanical integrity. For instance early designers often choose a material such as aluminum for the outer region and a very light material such as balsa wood for the inner region [41]. Modern sandwich structures typical use a stiff fiber composite (i.e. carbon fiber) as the outer material, and a very light Honey Comb matrix for the inner region [25]. The single most important design parameter with regard to the sandwich structure is the distance between the outer regions. The greater this distance the stiffer the structure will be. So, the ratio of the outer region thickness to the inner region thickness is optimized by the designer to provide as much stiffness as possible for a desired mass and total plate thickness. This kind of structure had been used in the aerospace industry for many decades [22],[23],[25].

The monocoque analogy takes advantage of this philosophy. It allows the analysis of rigidity without consideration of the inner region material. The only information about the inner region that impacts the overall stiffness of the sandwich structure is the distance it moves the outer regions away from each other. This allows flexural rigidity to take a very simple and useful form.

Ultimately the monocoque analogy is an estimation based calculation, as such it has limitations. Specifically, the outer region material cannot have material properties that are drastically ‘weaker’ than the inner region material, and the thickness of the inner region in relation to the thickness of outer region must fall into a certain usability criteria for a given application. It is important to note that the application of this sort of rigidity to reactor fuel plates may fall outside of the bounds of similar criteria provided in literature. This discrepancy can be seen in Carlsson and Kardomateas

[22] and Vinson's work [23]. This is because these authors focused on design applications that are not necessarily applicable to reactor fuel plates. Specifically, attention is directed towards optimizing the 'strength' of a sandwich structure for a case where the design variables and thicknesses are not fixed. These authors' design criteria work best in a case where the designer may choose from many different outer region materials. In applications directed towards reactor fuel plates this is not the case, typically the choice of inner region and outer region material has already been determined (i.e. aluminum and uranium-molybdenum).

This does not mean that the monocoque analogy is not applicable. It may still be used, but its applicability is dependent on the designers engineering judgment. Several test cases demonstrating the applicability of the monocoque analogy are provided in the results chapter.

3.2.2 Ideal Laminate Model

The ideal laminate model represents the full analytical solution to the flexural rigidity of a sandwich structure. Unlike the monocoque analogy, it takes into account information from the outer region as well as the inner region. It does not suffer from the same usability problems as the monocoque analogy, because it considers all portions of the sandwich structure. The ideal laminate flexural rigidity is shown below in equation (3.57).

$$D_{IL} = \frac{1}{3}\left(\frac{2E_{OR}}{\left(1-\nu_{OR}^2\right)}\left(\frac{3}{4}t_{IR}^2 t_{OR} + \frac{3}{2}t_{IR}t_{OR}^2 + t_{OR}^3 \right) + \frac{E_{IR}}{\left(1-\nu_{IR}^2\right)}\frac{t_{IR}^3}{4} \right) \tag{3.57}$$

The derivation of the rigidity term presented in (3.57) was initially performed by Vinson; he focused on lightweight structures for the aerospace industry [23]. It is important to note that Carlsson and Kardomateas' work is very similar to Vinson's work. In fact a large portion of both derivations are identical. The primary difference is that Vinson's work defines the regions of the sandwich at the interface between

regions. This is in contrast to Calsson and Kardomateas who define their regions from the centroid.

Note that Vinson concerned himself with fiber reinforced structures. As such he included terms to quantify thermoelasticity (i.e. thermal expansion) and hygrothermal effects (i.e. moisture absorption). This study is not concerned with such structures, so these terms have been omitted. Isotropic homogenous sandwich structures are the focus of this study, so the work below reflects this.

As mentioned the work below shares many similarities with the derivation of the monocoque analogy. In fact all of the steps from (3.25) to (3.35) are identical. These steps have been omitted from this section.

The derivation of the ideal laminate model diverges from that of the monocoque analogy, when the force resultants *N* and moment couples *M* are generated from the body in Figure 3-7. This is because the limits of integration with respect to *N* and *M* are at the surface of the *k*-th region. The force resultants are shown mathematically by equation (3.58), and the moment couples are given by equation (3.59).

$$\begin{bmatrix} N_x \\ N_y \\ N_{xy} \end{bmatrix}_k = \sum_{k=1}^{N} \int_{t_{k-1}}^{t_k} \begin{bmatrix} \sigma_x \\ \sigma_y \\ \sigma_{xy} \end{bmatrix}_k dz \tag{3.58}$$

$$\begin{bmatrix} M_x \\ M_y \\ M_{xy} \end{bmatrix}_k = \sum_{k=1}^{N} \int_{t_{k-1}}^{t_k} \begin{bmatrix} \sigma_x \\ \sigma_y \\ \sigma_{xy} \end{bmatrix}_k z dz \tag{3.59}$$

Equations (3.58) and (3.59) may be written in the form shown by equations (3.60) and (3.61), by inputting the values for stress and applying the one-dimensional case.

$$N = \sum_{k=1}^{N} \left(\int_{t_{k-1}}^{t_k} Q_k \varepsilon_x^0 dz + \int_{t_{k-1}}^{t_k} Q_k \kappa_x dz \right) \tag{3.60}$$

$$M = \sum_{k=1}^{N} \left(\int_{t_{k-1}}^{t_k} Q_k \varepsilon_x^0 z dz + \int_{t_{k-1}}^{t_k} Q_k \kappa_x z dz \right) \tag{3.61}$$

Because the material of each region is isotropic, Q_k must be a constant. In addition, the displacements *u* are not a function of *z*, and neither are their derivatives (i.e. strain ε_x^0). Finally, the curvature κ is not a function of *z*. These simplifications to the force resultants and moment couples allow a number of terms to be grouped outside of the integrals, yielding equation (3.62) and (3.63).

$$N = \sum_{k=1}^{N} \left(Q_k \varepsilon_x^0 \int_{t_{k-1}}^{t_k} dz + Q_k \kappa_x \int_{t_{k-1}}^{t_k} dz \right) \tag{3.62}$$

$$M = \sum_{k=1}^{N} \left(Q_k \varepsilon_x^0 \int_{t_{k-1}}^{t_k} z dz + Q_k \kappa_x \int_{t_{k-1}}^{t_k} z dz \right) \tag{3.63}$$

Recall that the sandwich plate in question is symmetric about the sandwich centerline of the plate thickness, and the outer regions are of equal thickness. This causes equations (3.62) and (3.63) to become uncoupled, where $[B] = 0 = [C]$. Also, equations (3.62) and (3.63) may be restated in their one-dimensional forms. As seen in equations (3.64) and (3.65).

$$N = A\varepsilon_x^0 + B\kappa \tag{3.64}$$

$$M = B\varepsilon_x^0 + D\kappa \tag{3.65}$$

Integrating equations (3.64) and (3.65), factoring out ε_x^0 and κ, and grouping relevant term yields the following very useful equation for *A*, *B*, and *D*.

Where *A* is the extensional stiffness given by equation (3.66).

$$A = \sum_{k=1}^{N} Q_k \left(t_k - t_{k-1} \right) \tag{3.66}$$

B is the elastic coefficient[10] given by equation (3.67).

$$B = \sum_{k=1}^{N} Q_k \left(t_k^2 - t_{k-1}^2 \right) \tag{3.67}$$

D is the flexural rigidity given by equation (3.68).

$$D = \frac{1}{3} \sum_{k=1}^{N} Q_k \left(t_k^3 - t_{k-1}^3 \right) \tag{3.68}$$

The relations for extensional stiffness and flexural rigidity, equations (3.67) and (3.68), are very useful in this study. They allow for calculation of extensional stiffness and flexural rigidity in one-dimension for *k* layers[11]. This assumes that each layer in the sandwich structure is symmetric with respect to its partner, isotropic, homogenous, the outer regions are identical in thickness and material properties, and that there is no slip at the interface. Equations (3.66) and (3.68) are now solved for a one-dimensional sandwich structure having three discrete layers that satisfies the assumptions listed above.

The stiffness term for the top and bottom outer regions are given by equation (3.69).

---

[10] As noted $B = 0$ in this case. It is shown for the sake of thoroughness.

[11] If this is extended for more than three layers, the indices *k* are only valid in factors of 2 (i.e. k=1,2,6, etc.). Refer to Vinson for further information concerning this [23].

$$Q_{OR} = Q_1 = Q_3 = \frac{E_{OR}}{\left(1-\nu_{OR}^2\right)} \tag{3.69}$$

The stiffness term for the inner region is given by equation (3.70).

$$Q_{IR} = Q_2 = \frac{E_{IR}}{\left(1-\nu_{IR}^2\right)} \tag{3.70}$$

Applying equation (3.66) for a sandwich plate with three discrete layers yields the extensional stiffness (3.71).

$$\begin{aligned} A = Q_{OR}\left(-\frac{t_{IR}}{2}-\left(-\frac{t_{IR}}{2}-t_{OR}\right)\right)+Q_{IR}\left(\frac{t_{IR}}{2}-\left(-\frac{t_{IR}}{2}\right)\right) \\ +Q_{OR}\left(\left(\frac{t_{IR}}{2}+t_{OR}\right)-\frac{t_{IR}}{2}\right) \end{aligned} \tag{3.71}$$

Combining equations (3.69), (3.70), and (3.71) yields the extensional stiffness for the ideal laminate model (3.72).

$$A_{IL} = 2Q_{OR}t_{OR} + Q_{IR}t_{IR} = \frac{2E_{OR}}{\left(1-\nu_{OR}^2\right)}t_{OR} + \frac{E_{IR}}{\left(1-\nu_{IR}^2\right)} \tag{3.72}$$

Applying equation (3.68) for a sandwich plate with three discrete regions results in the following relation for flexural rigidity (3.73).

$$\begin{aligned} D = \frac{1}{3}Q_{OR}\left(\left(-\frac{t_{IR}}{2}\right)^3-\left(-\frac{t_{IR}}{2}-t_{OR}\right)^3\right)+\frac{1}{3}Q_{IR}\left(\left(\frac{t_{IR}}{2}\right)^3-\left(-\frac{t_{IR}}{2}\right)^3\right) \\ +\frac{1}{3}Q_{OR}\left(\left(\frac{t_{IR}}{2}+t_{OR}\right)^3-\left(\frac{t_{IR}}{2}\right)^3\right) \end{aligned} \tag{3.73}$$

Combining equations (3.69), (3.70), and (3.73) yields the flexural rigidity for the ideal laminate case (3.57).

$$D_{IL} = \frac{1}{3}\left(\frac{2E_{OR}}{\left(1-\nu_{OR}^2\right)}\left(\frac{3}{4}t_{IR}^2 t_{OR} + \frac{3}{2}t_{IR}t_{OR}^2 + t_{OR}^3 \right) + \frac{E_{IR}}{\left(1-\nu_{IR}^2\right)}\frac{t_{IR}^3}{4} \right) \tag{3.57}$$

Equation (3.57) is the complete analytical solutions for the flexural rigidity of a sandwich structure, derived from a general stress state (i.e. first principles). Throughout this work, it will be referred to as the ideal laminate model. It does not have the same usability and applicability limitations as the monocoque analogy. It will be shown, in subsequent sections that the ideal laminate model will consistently predict the flexural rigidity of a sandwich structure regardless of the dimensions of the inner or outer region.

3.3 Summary of Critical Flow Velocities and Critical Dynamic Pressures

This section presents the final formulation of critical flow velocity and critical dynamic pressure using the monocoque analogy and the ideal laminate model. These are presented concisely, and organized by edge boundary condition. The case in which both edge boundaries are clamped is denoted as “Clamped-Clamped”. The case in which one edge is clamped and one is simply supported is denoted as “Clamped-Simply Supported”. The case in which both edges simply supported is denoted as “Simply Supported-Simply Supported”. Equations (3.74) through (3.79) represent the relations developed for predicting the critical flow velocity using the monocoque analogy and the ideal laminate model for all three edge boundary conditions, while equations (3.80) though (3.85) present these same relations as critical dynamic pressure.

Critical Flow Velocities:

Clamped-Clamped Monocoque Analogy:

$$V_{cr-mon} = \left(\frac{h}{\rho L^4} \right)^{1/2} \left(90 \left(t_{IR} + t_{OR} \right)^2 t_{OR} \left(\frac{E_{OR}}{\left(1 - \nu_{OR}^2 \right)} \right) \right)^{1/2} \tag{3.74}$$

Clamped-Clamped Ideal Laminate:

$$V_{cr-IL} = \left(\frac{h}{\rho L^4} \right)^{1/2} \left(60 \left(\frac{2E_{OR}}{\left(1 - \nu_{OR}^2 \right)} \left(\frac{3}{4} t_{IR}^2 t_{OR} + \frac{3}{2} t_{IR} t_{OR}^2 + t_{OR}^3 \right) \right) + \frac{E_{IR}}{\left(1 - \nu_{IR}^2 \right)} \left(\frac{t_{IR}^3}{4} \right) \right)^{1/2} \tag{3.75}$$

Clamped-Simply Supported Monocoque Analogy:

$$V_{cr-mon} = \left(\frac{h}{\rho L^4} \right)^{1/2} \left(40 \left(t_{IR} + t_{OR} \right)^2 t_{OR} \left(\frac{E_{OR}}{\left(1 - \nu_{OR}^2 \right)} \right) \right)^{1/2} \tag{3.76}$$

Clamped-Simply Supported Ideal Laminate:

$$V_{cr-IL} = \left(\frac{h}{\rho L^4} \right)^{1/2} \left(\frac{80}{3} \left(\frac{2E_{OR}}{\left(1 - \nu_{OR}^2 \right)} \left(\frac{3}{4} t_{IR}^2 t_{OR} + \frac{3}{2} t_{IR} t_{OR}^2 + t_{OR}^3 \right) \right) + \frac{E_{IR}}{\left(1 - \nu_{IR}^2 \right)} \left(\frac{t_{IR}^3}{4} \right) \right)^{1/2} \tag{3.77}$$

Simply Supported-Simply Supported Monocoque Analogy:

$$V_{cr-mon} = \left(\frac{h}{\rho L^4} \right)^{1/2} \left(15\left(t_{IR} + t_{OR}\right)^2 t_{OR} \left(\frac{E_{OR}}{\left(1-\nu_{OR}^2\right)} \right) \right)^{1/2} \tag{3.78}$$

Simply Supported-Simply Supported Ideal Laminate:

$$V_{cr-IL} = \left(\frac{h}{\rho L^4} \right)^{1/2} \left(10 \left(\frac{2E_{OR}}{\left(1-\nu_{OR}^2\right)} \left(\frac{3}{4} t_{IR}^2 t_{OR} + \frac{3}{2} t_{IR} t_{OR}^2 + t_{OR}^3 \right) \right) + \frac{E_{IR}}{\left(1-\nu_{IR}^2\right)} \left(\frac{t_{IR}^3}{4} \right) \right)^{1/2} \tag{3.79}$$

Critical Dynamic Pressures:

Clamped-Clamped Monocoque Analogy:

$$q_{cr-mon} = \left(\frac{h}{L^4}\right)\left(90\left(t_{IR}+t_{OR}\right)^2 t_{OR}\left(\frac{E_{OR}}{\left(1-\nu_{OR}^2\right)}\right)\right) \tag{3.80}$$

Clamped-Clamped Ideal Laminate:

$$q_{cr-IL} = \left(\frac{h}{L^4}\right)\left(60\left(\frac{2E_{OR}}{\left(1-\nu_{OR}^2\right)}\left(\frac{3}{4}t_{IR}^2 t_{OR}+\frac{3}{2}t_{IR}t_{OR}^2+t_{OR}^3\right)\right.\right. \\ \left.\left.+\frac{E_{IR}}{\left(1-\nu_{IR}^2\right)}\left(\frac{t_{IR}^3}{4}\right)\right)\right) \tag{3.81}$$

Clamped-Simply Supported Monocoque Analogy:

$$q_{cr-mon} = \left(\frac{h}{L^4}\right)\left(40\left(t_{IR}+t_{OR}\right)^2 t_{OR}\left(\frac{E_{OR}}{\left(1-\nu_{OR}^2\right)}\right)\right) \tag{3.82}$$

Clamped-Simply Supported Ideal Laminate:

$$q_{cr-IL} = \left(\frac{h}{L^4}\right)\left(\frac{80}{3}\left(\frac{2E_{OR}}{\left(1-\nu_{OR}^2\right)}\left(\frac{3}{4}t_{IR}^2 t_{OR}+\frac{3}{2}t_{IR}t_{OR}^2+t_{OR}^3\right)\right.\right. \\ \left.\left.+\frac{E_{IR}}{\left(1-\nu_{IR}^2\right)}\left(\frac{t_{IR}^3}{4}\right)\right)\right) \tag{3.83}$$

Simply Supported-Simply Supported Monocoque Analogy:

$$q_{cr-mon} = \left(\frac{h}{L^4}\right)\left(15\left(t_{IR}+t_{OR}\right)^2 t_{OR}\left(\frac{E_{OR}}{\left(1-\nu_{OR}^2\right)}\right)\right) \tag{3.84}$$

Simply Supported-Simply Supported Ideal Laminate:

$$q_{cr-IL} = \left(\frac{h}{L^4}\right)\left(10\left(\frac{2E_{OR}}{\left(1-\nu_{OR}^2\right)}\left(\frac{3}{4}t_{IR}^2 t_{OR}+\frac{3}{2}t_{IR}t_{OR}^2+t_{OR}^3\right)+\frac{E_{IR}}{\left(1-\nu_{IR}^2\right)}\left(\frac{t_{IR}^3}{4}\right)\right)\right) \tag{3.85}$$

3.4 Closing

Two models which predict what has been termed plate collapse for flat laminated plates were developed herein. These models predict the flow velocity and/or dynamic pressure at which this phenomenon occurs. The flexural rigidity for a laminated plate was then derived, using two methods, from a general stress state. The first was termed the monocoque analogy, which relies primarily on the mechanical contribution of the outer region material. The second was termed the ideal laminate model in which the mechanical contributions of all regions are considered. These flexural rigidity terms were then incorporated into the aforementioned models yielding the critical flow velocity and/or critical dynamic pressure for a laminated plate.

4 RESULTS AND DISCUSION

This chapter presents and describes several test cases, which highlight the robustness and applicability of the ideal laminate model along with the monocoque analogy. The boundary conditions for each test case are detailed, and discussions of each test case's results are presented. In addition, a comparison to previous experimental work is provided and demonstrates relatively good agreement throughout.

4.1 Test Cases

Three 'Test Cases' are described and performed in comprehensive detail. These test cases are intended to qualitatively and quantitatively demonstrate the robustness and applicability of the models developed herein. For all test cases the clamped-clamped edge boundary condition was employed.

4.1.1 Test Case 1- Sensitivity Due to Region Thicknesses

As the thickness of the inner and/or outer region is varied, the relative percent of load carried by the respective region will change. This presents a liability for the monocoque analogy. The monocoque analogy, assumes that the outer region carries a significant amount of the load; so much so that the overall stiffness of the plate is approximated by the outer region only. Thus the mechanical contribution of the outer region is used solely to approximate the plate's flexural rigidity, and the inner region is ignored. This is generally a safe assumption under most cases where the sandwich structure is sufficiently thin that it may be viewed as a laminated shell[12]. Yet even for a thin sandwich plate, certain cases exist in which the applicability of the monocoque analogy may be questioned. These cases arise, as the thickness of the inner and outer regions is varied.

To illustrate this consider a sandwich plate having three discrete regions (as presented in Figure 3-5) with constant total thickness. Assume that this plate has three discrete

[12] A shell is simply a thin three dimensional elastic body in space. A thin flat plate is a shell.

regions with equal materials properties. Also, consider a homogenous plate (one region) with a thickness equal to the total thickness of the sandwich plate. Assuming that each layer in the sandwich is perfectly bound to one another, logic dictates that a valid model to predict critical flow velocity for a sandwich plate would predict the same values as the homogenous case. Test case 1 compares the laminate models' ability to predict the critical flow velocity of a homogenous plate as compared against Miller's model.

In this test case, the relative thickness of the inner and outer region is varied while the total thickness is held constant. The boundary conditions used are presented in Table 4-1.

Table 4-1: Test Case 1 boundary conditions

Parameter	Inner Region	Outer Region
Thickness [%]	0 – 100	50 – 0
Ratio span-width to total thickness [#]	80	
Total thickness [mm]	1	
Young's Modulus [MPa]	1E6	
Poisson's Ratio [#]	0.33	
Channel height to total thickness ratio [#]	1	
Fluid density [kg/m^3]	1E3	

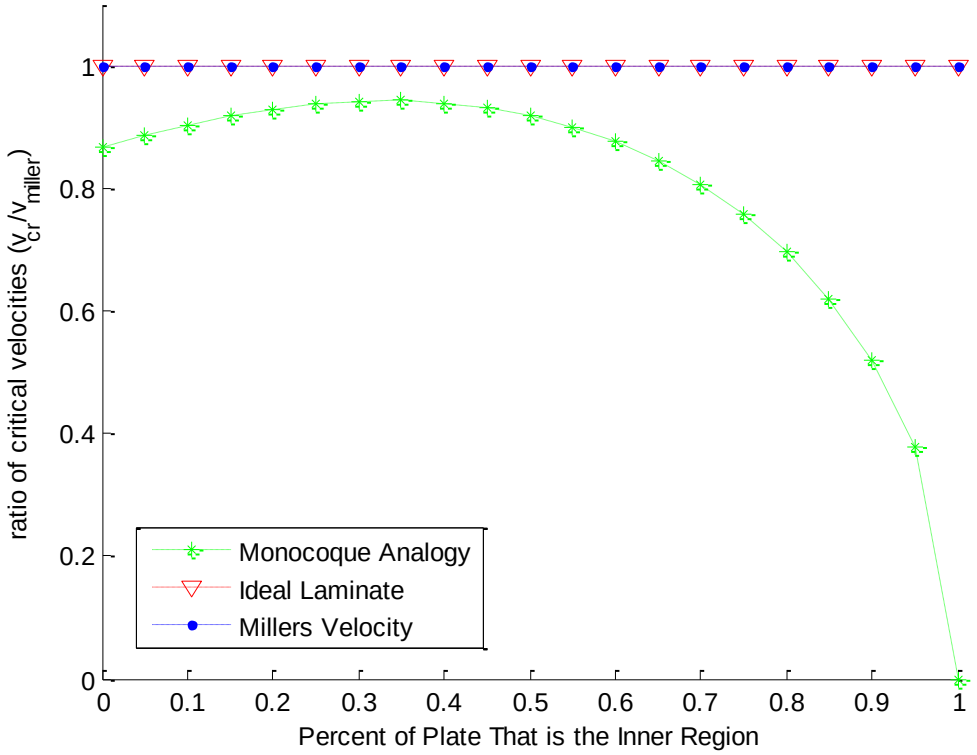

Figure 4-1: Critical flow velocity ratio versus percent inner region thickness

In Figure 4-1 the y-axis represents the relative percent that the inner region occupies, while the x-axis presents the ratio of critical flow velocity predicted by each model to that predicted by Miller's method.

When Compared against Miller's method, the ideal laminate model precisely predicts the critical flow velocity through the entire range of varied thicknesses. This is expected as the mathematical formulation, although including a number of assumptions, is derived on the basis that the stress loading imposed by the hydraulic domain is carried in all the regions of the plate regardless of each region's thickness.

In contrast, the monocoque analogy provides a best estimate between 20 and 50 percent, with the most accurate prediction occurring when each layer is equal (i.e. the

inner layer occupies approximately 33 percent of the total thickness). The variance in the monocoque analogy's ability to predict critical flow velocity is due to the load being shifted from the outer region material to the inner region material as the thickness of each region is changed. The monocoque analogy does not consider the rigidity of the core material. No mechanical properties or geometric properties are taken into the monocoque analogy for the inner region material, as seen in equation (3.24). This causes the monocoque analogy to significantly under predict the critical flow velocity as the inner region becomes thick. In addition, as the outer regions become thick (i.e. inner plate region thickness is less than 33 percent), the monocoque analogy also under predicts the critical flow velocity. This is driven by the fact that the geometric properties of the outer region do not properly scale as the laminate plate approaches the geometry of the homogenous plate. This may be observed by comparing the flexural rigidities for a homogenous plate given by equation (3.23) and the flexural rigidity given by the monocoque analogy shown in equation (3.24).

Additionally an alternative perspective may be taken, which demonstrate the monocoque analogy's inability to predict the critical flow velocity as the inner regions thickness approaches zero. This is demonstrated by utilizing the parallel axis theorem to derive the flexural rigidity of the monocoque analogy. In which the parallel axis theorem is modified, by assuming that the second area moment of inertia for each region is negligible. For this assumption to hold true, each region must have some thickness which is not true as the inner region percentage approaches zero. A complete derivation of this is shown in Appendix B.

4.1.2 Test Case 2- Sensitivity Due to Total Thickness

As the total thickness of a sandwich plate increase, more load is carried by the inner region. The transfer of load results in the monocoque analogy and the ideal laminate model gradually diverging as the total thickness increases. To be specific the monocoque analogy will under predict the critical flow velocity as the total thickness increases.

As with the previous test case, the critical flow velocity for a plate with three discrete layers of equal material properties was calculated using both models and compared to the critical flow velocity for a homogenous plate predicted using Miller's method. The boundary conditions used for Test Case 2 are shown in Table 4-2.

Table 4-2: Test Case 2 boundary conditions

Parameter	Inner Region	Outer Region
Thickness [%]	33.3	33.3
Total thickness [mm]	1-10	
Span-width [mm]	80	
Young's Modulus [MPa]	1E6	
Poisson's Ratio [#]	0.33	
Channel height to total thickness ratio [#]	1	
Fluid density [kg/m^3]	1E3	

Figure 4-2 shows how the monocoque analogy gradually becomes less accurate as the total thickness of the plate is increased. A shown in Figure 4-1, there will always be a small discrepancy between the monocoque analogy and ideal laminate model. This discrepancy increases as the total thickness of the plate increases, due to the monocoque analogy's inability to quantify effects occurring in the inner region of the plate.

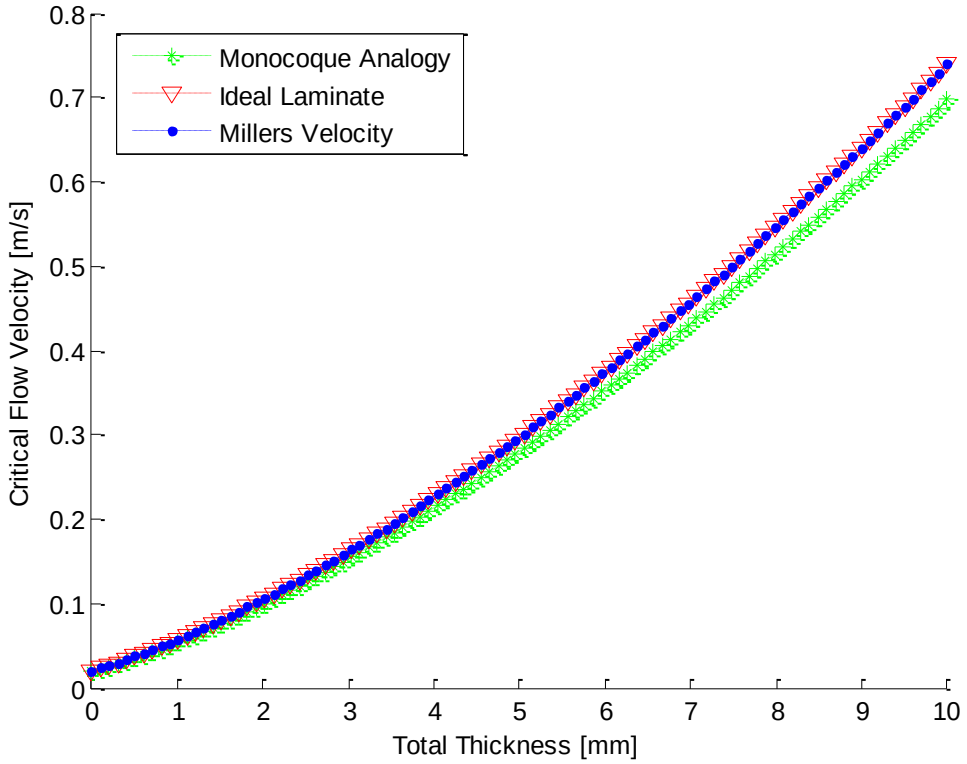

Figure 4-2: Critical flow velocity versus total thickness

4.1.3 Test Case 3- Sensitivity Due to Material Composition

The material composition of each region may also adversely affect each model's ability to accurately predict critical flow velocity. An actual fuel plate will have cladding material and fueled material; the material properties of each have profound effects on the plate's resistance to flow induced instabilities. In the case of high performance research reactor fuel plates the Young's Modulus of the fuelled region is larger than that of the clad [51]. In such a case, the inner region will contribute more to the overall rigidity of the plate than if it were comprised of a 'weaker' material. Each model's sensitivity to a change in the material composition of each region is

compared in this test case. The boundary conditions used for Test Case 3 are given in Table 4-3

Table 4-3: Test Case 3 boundary conditions

Parameter	Inner Region	Outer Region
Thickness [%]	33.3	33.3
Ratio span-width to total thickness [#]	80	
Total thickness [mm]	1	
Ration of Young's Moduli (E_{IR}/E_{OR}) [MPa]	1E-3 to 1E3	
Poisson's Ratio [#]	0.33	
Channel height to total thickness ratio [#]	1	
Fluid density [kg/m^3]	1E3	

Figure 4-3 shows the sensitivity of each model to changes in the material composition of the inner region. As before the critical flow velocity for each model is compared to Miller's method. Miller's method was calculated by using the material properties for the outer region, and the total thickness of the laminated plate. The thickness of each region in the laminated plate was assumed to be one-third the total thickness of the plate. As shown in Figure 4-3 the ratio of critical flow velocities is compared to the ratio of inner and outer region Young's Moduli.

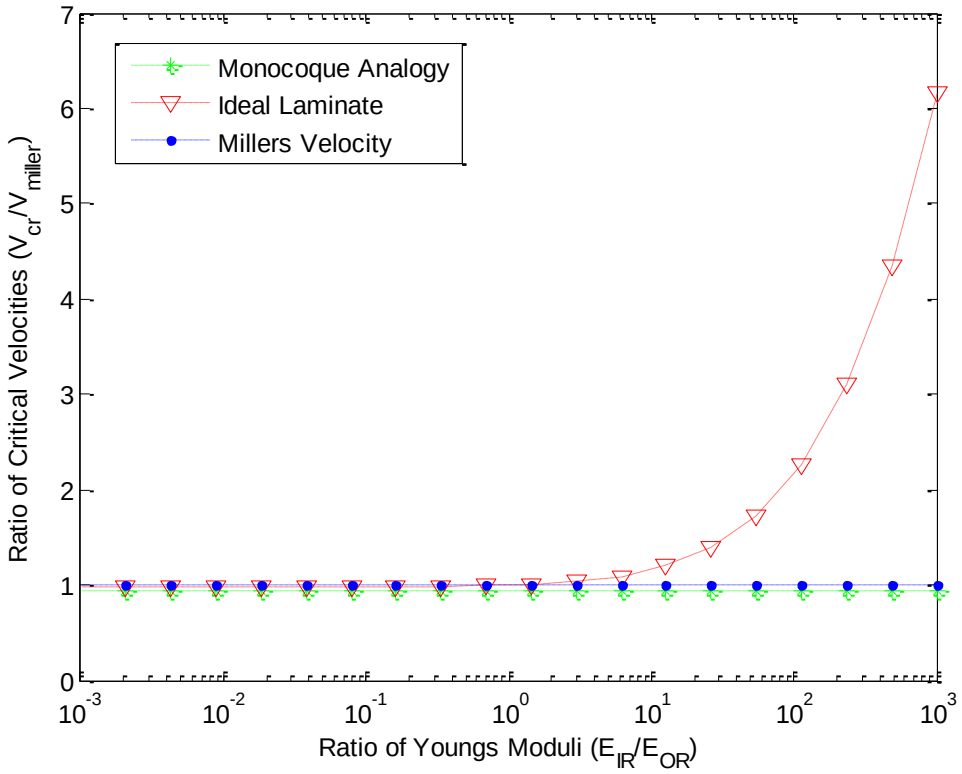

Figure 4-3: Critical velocity ratio vs. Young's Moduli ratio

Figure 4-3 shows that as the inner regions Young's Moduli increases the accuracy of the monocoque analogy relative to that of the ideal laminate case is diminished. In addition, simply using the material information for the clad material in Miller's method is also unacceptable in this case. This is because neither method considers the contribution of the inner region to the rigidity of the structure. Notice that all models show close agreement until the ratio of Young's Moduli reaches unity. Beyond unity the ideal laminate model performs well, while the monocoque analogy and Miller's method becomes less accurate. Clearly, the ideal laminate model predicts the most representative critical flow velocity.

Additional information for this test case, in which each region thickness is varied as the ratio of Young's Moduli is varied, is supplied in Appendix C.

4.2 Model Comparison Against Experimental Data

The models presented herein, are compared to previous experimental work. Currently, there exists no relevant available experimental data on critical flow velocity of laminated plates, however, numerous studies have been performed on this subject while employing homogeneous plates. While it is not ideal to compare a laminate model to homogenous model, it has been shown in the previous test cases that such a comparison is valid under certain conditions.

Several authors provide critical flow velocity data for homogenous plates. Most applicable to this study is the work of Zabriskie [16] and Smith [12]; these authors included test results for failure of plates under static conditions. Of the two authors, Smith's data was determined to be most applicable. This is because Smith conducted tests for four separate materials, and presented the experimental variability of results for each test. In contrast, Zabriskie did not provide any information concerning the variability of his measured results. There are some undesirable aspects to Smith's work, however; (1) the error associated with some of his experimental test cases is very large, and (2) the method he choose in conveying his results made it very difficult to accurately extract usable information from his work. Relatively large error and difficulty in reproducibility is not uncommon among critical flow velocity and critical dynamic pressure studies [20], [26], and only highlights the need for modern experimental facilities such as the Oregon State University Hydro Mechanical Fuel Test Facility.

Smith's work focused on small beams of lead, aluminum, copper, and steel. Of the materials tested lead was the least stiff material and steel was the stiffest. The test facility Smith used was designed to circulate helium or air as the working fluid. The data set chosen for comparison was taken from figure 6, in Smith's study [12]. This data set compared the critical dynamic pressure at beam failure, against a material parameter for each beam. The critical dynamic pressure for the monocoque analogy may be obtained from equation (3.80), given that both edge boundary conditions are

clamped. Likewise, the critical dynamic pressure for the ideal laminate model with clamped edges may be obtained from equation (3.81). As with the previous homogenous examples, the laminate models were compared to Miller's method for a homogenous plate. Table 4-4 outlines the boundary conditions for each model which reflects those tested by Smith.

Table 4-4: Comparison against experimental work boundary conditions

Parameter	Inner Region		Outer Region	
Thickness for laminated region [%]	33.3		33.3	
Total plate thickness [mm]	0.508			
Plate span width [cm]	5.08			
Flow channel height [mm]	1.62			
	Lead	Aluminum	Copper	Steel
Young's Modulus [GPa]	15.9	69.0	117	210
Poisson's Ratio [#]	0.44	0.33	0.33	0.27

Figure 4-4 compares the predicted critical dynamic pressure, to Smith's observed critical dynamic pressure at plate failure. It should be noted that as in Test Case 1 the results predicted by Miller's method and the ideal laminate model agree perfectly due to the homogenous nature of the plates under consideration, while the monocoque analogy presents results that are slightly less than that of the other two models.

Figure 4-4, shows the results compared to Smith's data for a plate with both edge boundaries clamped. This is the most mechanically rigid case. As is seen, there is great variability in Smith's data, and the critical dynamic pressure predicted by the models is slightly greater than the average presented by Smith for each material.

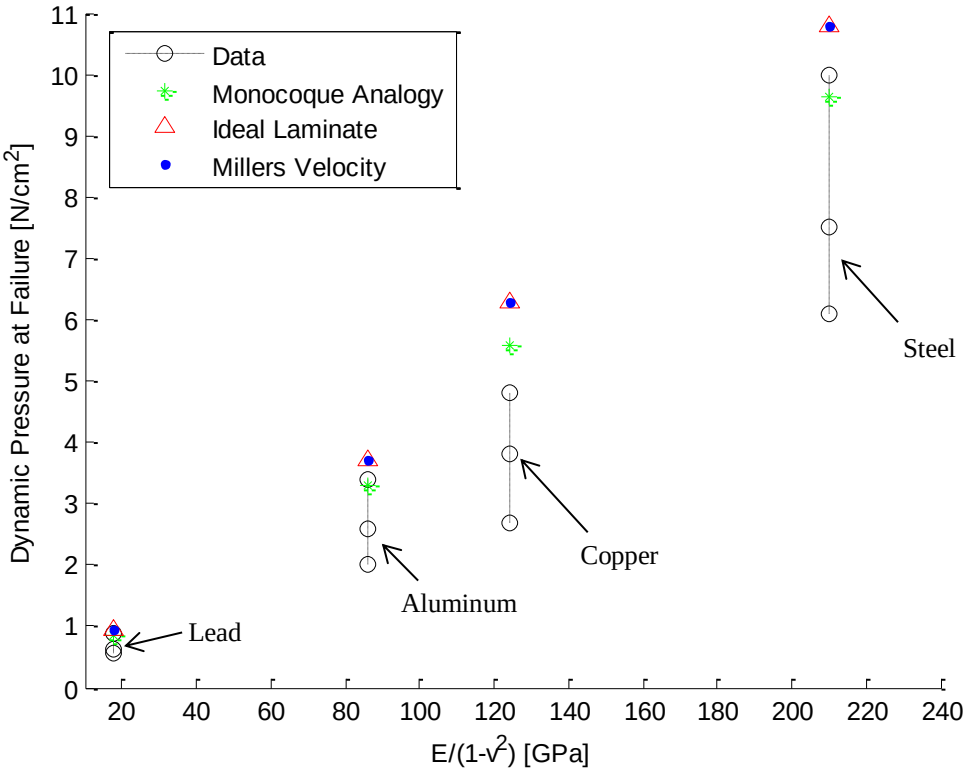

Figure 4-4: Clamped-Clamped edge boundary condition

Although each model's ability to predict critical dynamic pressure trends with that observed by Smith, the validity of this comparison is hard to gauge, because there is significant variability in Smith's data. Also, Smith chose to quantify plate failure when a plate's deflection is greater than or equal to 0.254 mm. This definition of plate failure can be debated. Recall, the point of failure when using critical flow velocity or critical dynamic pressure does not refer to a specific deflection. Plate collapse, as previously defined above, is the point at which the plate has deflected to such an extent that a linearized beam deflection model is no longer acceptable to characterize the phenomena at hand.

5 CONCLUSION

This study investigates two methods for determining the critical flow velocity for a pair of laminate plates. The objective is accomplished by incorporating a flexural rigidity term into the formulation of critical flow velocity originally derived by Miller, and employing sandwich structure theory to determine the rigidity term.

The flexural rigidity term is derived in two ways. The first is termed the monocoque analogy, and only considers the mechanical contribution of the outer regions material to a plate's flexural rigidity. The second considers every layer's contribution to flexural rigidity. Both are derived from a general stress state.

The methods presented herein, allow for a single simple calculation to be preformed in order to predict the flow velocity or dynamic pressure that causes 'plate collapse'. The simplicity of these methods is intended to provide designers with a useful tool which compliments other forms of analysis.

The final outcome of this study results in the developing of a single equation for each of three different edge boundary conditions which reliably and comprehensively predicts the onset of plate collapse.

This monocoque analogy, acknowledges that the inner region of the laminate plate provides insignificant mechanical stiffness to the laminate, and subsequently ignores this region. This result is presented in equations (3.74), (3.76), and (3.78). These equations may be simply reformulated into one equation utilizing the constant k which shall be termed the edge boundary constant. This constant assumes a value of 90 when both edges are clamped, 40 when one edge is clamped and one is simply supported, and 15 when both edges are simply supported. The final form of the monocoque analogy is shown in equation (5.1).

$$V_{cr-mon} = \left(\frac{h}{\rho L^4}\right)^{1/2}\left(k\left(t_{IR}+t_{OR}\right)^2 t_{OR}\left(\frac{E_{OR}}{\left(1-\nu_{OR}^2\right)}\right)\right)^{1/2} \tag{5.1}$$

The ideal laminate model, makes fewer assumptions about the mechanical contribution of each region, and subsequently includes the mechanical contribution for all regions. It is shown to be robust in comparison to the monocoque analogy, by Test Cases 1, 2, and 3. This model is presented in equations (3.75), (3.77), and (3.79). These equations may also be simplified by including an edge boundary constant *k*. The edge boundary constant assumes the value of 60 when both edges are clamped, 80/3 when one edge is clamped and one is imply supported, and 10 if both edges are simply supported. The final form of the ideal laminate model is shown in equation (5.2).

$$V_{cr-IL} = \left(\frac{h}{\rho L^4}\right)^{1/2}\left(k\left(\frac{2E_{OR}}{\left(1-\nu_{OR}^2\right)}\left(\frac{3}{4}t_{IR}^2 t_{OR}+\frac{3}{2}t_{IR}t_{OR}^2+t_{OR}^3\right)\right)+\frac{E_{IR}}{\left(1-\nu_{IR}^2\right)}\left(\frac{t_{IR}^3}{4}\right)\right)^{1/2} \tag{5.2}$$

5.1 Assumptions and Applicability

The formulation of critical flow velocity presented in this thesis includes several assumptions, listed below:

- The plate is initially un-deformed and perfectly flat, deforms symmetrical about its neutral axis, and its deflections are small enough to allow the use of the Euler-Bernoulli beam theorem.

- The fluid is incompressible and isothermal, and the flow is steady and uniform for the flow channel at any given point along the channel length.

- Internal shear in the plate is considered negligible, and the plane stress assumption is applied.

- The plate edge supports are perfectly rigid.

- The plate behaves as a wide beam.

- The plate is a sandwich structure, which is symmetric with one inner region and two out regions.

- The regions of the sandwich plate are isotropic, linearly elastic, have perfect mechanical constants (i.e. Young's Modulus, Poison's Ratio), and no slip occurs at the interface of the regions.

The applicability of each model presented herein, has also been thoroughly explored in previous chapters. The ideal laminate model presented in equation (5.2), was shown to be robust, and consistently produced valid results. The monocoque analogy presented in equation (5.1), showed some applicability issues when the percentage of the inner region increased beyond 50 percent or decreased below 20 percent with ideal range of approximately 33 percent, this is illustrated in Figure 4-1. Also, the monocoque analogy may lose some fidelity if the sandwich plate becomes very thick. Finally, its applicability is also poor in cases where the inner regions Young's modulus[13] becomes of the order or greater than outer regions, this is shown in Figure 4-2

5.2 Future Work

Presently, there is a lack of highly robust experimental data for flow induced deflections of laminated plates under hydraulic loading. This makes validation of any theoretical model, very difficult. While previous experimental work does exist for

[13] Young's modulus or the material parameter $E/(1-\nu^2)$

homogenous plates, this work often times does not provide detailed descriptions of the materials used and generally lacks statistical information concerning the error, confidence, and uncertainty on the measured data.

In addition to experimental work, theoretical work may also be expanded upon by applying sandwich structure theory to previous models that focused solely on homogenous plate. There currently exists static and dynamic models for plates with many different geometries, in which the laminated nature of the plate may be included by applying sandwich structure theory in the same fashion as it was done herein.

6 BIBLIOGRAPHY

[1] W. R. Marcum, “OSU HMFTF-Facility Description,” 2012.

[2] “Global Threat Reduction Initiative – Conversion Program: Reduced Enrichment for Research and Test Reactors (RERTR).” 2010.

[3] P. Leventhal and A. Kuperman, “RERTR At The Crossroads: Success or Demise?,” Washington DC, 1995.

[4] A. Loukianova and C. Hansell, “LEVERAGING U.S. POLICY FOR A GLOBAL COMMITMENT TO HEU ELIMINATION,” *The Nonproliferation Review*, vol. 15, no. 2, 2008.

[5] Alexander Glaser and F. N. von Hippel, “Global Cleanout: Reducing the Threat of HEU-Fueled Nuclear Terrorism,” *Arms Control Today*, 2006.

[6] P. Staples, “Reduced Enrichment for Research and Test Reactors Program.” Office of Global Nuclear Material Threat Reduction (NA-212), National Nuclear Security Administraition, 2006.

[7] W. R. Marcum, “OSU HMFTF Fuels Development Program-Matrix Test Plan,” 2012.

[8] International Atomic Energy Agency IAEA-TECDOC-643, “Research Reactor Core Conversion Guidebook.”

[9] International Atomic Energy Agency IAEA-TECDOC-1345, “Fuel Failure in Water Reactors: Causes and Mitigation.”

[10] R. A. Knief, *Nuclear Engineering: Theory and Technology of Commercial Nuclear Power*. American Nuclear Society, 2008.

[11] D. R. Miller, “Critical Flow Velocities for Collapes of Reactor Parallel-Plate Fuel Assemblies,” Schenectady, New York.

[12] R. L. Smith, “Dynamic Pressure Limits for Flat Plates as Related to Nuclear Fuel Elements,” Washington DC, 1968.

[13] M. W. Wambsganss, “Second-Order Effects as Related to Critical Coolant Flow Velocities in Reactor Parallel Plate Fuel Assemblies,” *Nuclear Engineering and Design*, vol. 5, pp. 268–276, 1967.

[14] R. B. Johansson, “Hydraulic Instability of Reactor Parallel Plate Fuel Assemblies,” in *Nuclear Engineering Science Conference*, 1960, p. paper # 57.

[15] W. R. Marcum, “Predicting Mechanical Instability of a Cylindrical Plate under Axial Flow Conditions,” Oregon State University, 2010.

[16] W. L. Zabriskie, “An Experimental Evaluation of Critical Flow Velocity Formulas for Parallel Plate Assemblies,” 1958.

[17] F. P. Beer, E. R. J. Johnston, J. T. Dewolf, and D. F. Mazurek, *Mechanics of Materials*, Fifth ed. Boston: McGraw-Hill, 2006.

[18] B. Goodwine, *Engineering Differential Equations: Theory and Applications*. Springer, 2011.

[19] W. C. Young and R. G. Budynas, *Roark’s Formulas For Stress and Strain*, Seventh ed. New York: McGraw-Hill, 2002.

[20] R. D. Groninger and J. J. Kane, “Flow Induced Deflections of Parallel Flat Plates,” *Nuclear Science and Engineering*, vol. 16, pp. 218–226, 1963.

[21] D. M. Wachs, C. R. Clark, and R. J. Dunavant, “Conceptual Process Description for the Manufacture of Low-Enriched Uranium-Molybdenum Fuel,” 2008.

[22] L. A. Carlsson and G. A. Kardomateas, *Structural and Failure Mechanics of Sandwich Composites*, vol. 121. Dordrecht: Springer Netherlands, 2011.

[23] J. R. Vinson, *The Behavior of Sandwich Structures of Isotropic and Composite Materials*. Lancaster, PA: Technomic Pub. Co., 1999.

[24] E. A. Avallone and T. Baumeister, *Mark’s Standard Handbook for Mechanical Engineers*, Ninth ed. New York: McGraw-Hill Book Company, 1987.

[25] J. N. Reddy, *Mechanics of Laminated Composite Plates: Theory and Analysis*. CRC Press, 1997.

[26] W. K. Stromquist and O. Sisman, “High Flux Reactor Fuel Assemblies Vibration and Water Flow,” 1948.

[27] R. L. Doan, “The Engineering Test Reactor-A Status Report,” *Nucleonics*, vol. 16, 1958.

[28] R. G. Budynas, *Advanced Strength and Applied Stress Analysis*. New York: McGraw-Hill Book Company, 1977.

[29] F. B. Seely and J. O. Smith, *Advanced Mechanics of Materials*, Second ed. New York: John Wiley & Sons, 1952.

[30] W. L. Zabriskie, "An Experimental Evaluation of the Effect of Length-to-Width Ratio on the Critical Flow Velocity of Single Plate Assemblies," 1959.

[31] J. J. Kane, "The Effect of Inlet Spacing Deviations on the Flow-Induced Deflections of Parallel Plates," *Nuclear Science and Engineering*, vol. 15, no. 3, pp. 305–308, 1963.

[32] G. E. Smissaert, "Static and Dynamic Hydroelastic Instabilities in MTR-Type Fuel Elements Part I: Introduction and Experimental Investigation," *Nuclear Science and Engineering*, vol. 7, p. 11, 1968.

[33] Y. T. Kim and H. A. Scarton, "Flow-Induced Bending ofRectangular Plates," *Journal of Applied Mechanics*, vol. 44, 1977.

[34] M. Ho, G. Hong, and A. N. F. Mack, "Experimental Investigation of Flow-Induced Vibration in a Parallel Plate Reactor Fuel Assembly," in *15th Australian Fluid Mechanics Conference*, 2004.

[35] J. M. Whitney, *Structural Analysis of Laminated Anisotropic Plates*. Technomic Pub. Co., 1987.

[36] G. S. Gough, C. F. Elam, and N. A. DeBruyne, "The Stabilisation of a Thin Sheet by a Continuous Supporting Medium," *Journal of the Royal Aeronautical Society*, vol. 44, pp. 12–43, 1940.

[37] D. Williams, D. M. A. Leggett, and H. G. Hopkins, "Flat Sandwich Panels Under Compressive End Loads," 1941.

[38] C. Libove and S. B. Batdorf, "A General Small-Deflection Theory For Flat Sandwich Plates," Washington DC, 1948.

[39] E. Reissner, "Finite Deflections of Sandwich Plates," *Journal of Aeronautical Sciences*, 1948.

[40] N. J. Hoff and S. E. Mautner, "Bending and Buckling of Sandwich BEams," *Journal of Aeronautical Sciences*, 1948.

[41] N. J. Hoff, “Bending and Buckling of Rectangular Sandwich Plates,” Washington DC, 1950.

[42] A. C. Eringen, “Bending and Buckling of Rectangular Sandwich Plates,” in *Proceedings of the first U.S. National Congress of Applied Mechanics; held at Illinois Institute of Technology, Chicago, Illinois*, 1951, pp. 381–390.

[43] W. S. Ericksen, “Effects of Shear Deformation in the Core of a Flat Rectangular Panel: Compressive Buckling of Sanwich Panels having Dissimilar Facings of Unequal Thickness,” 1958.

[44] M. J. Yan and E. H. Dowell, “Elastic Sandwich Beam or Plate Equations Equivalent to Classical Theory,” *Journal of Applied Mechanics*, vol. 41, pp. 526–527, 1974.

[45] P. V. Cavallaro and J. Melvin, “Structural Analysis & Experimental Activities Supporting The Design of a Lightweight Rigid-Wall Mobile Shelter,” 2008.

[46] A. P. Boresi and R. J. Schmidt, *Advanced Mechanics of Materials*, Sixth rd. John Wiley & Sons, 2003.

[47] C. R. Luttrell, “Finite Element Analysis of Advanced Nautron Source Fuel Plates,” 1995.

[48] R. W. Fox and A. T. McDonald, *Intorduction to Fluid Mechanics*, Fouth ed. New York: John Wiley & Sons, 1992.

[49] Munson, Young, Okiishi, and Huebsch, *Fundamentals of Fluid Mechanics*, Sixth ed. John Wiley & Sons, 2009.

[50] L. D. Landau and E. M. Lifshitz, *Course of Theoretical Physics. - 7: Theory of Elasticity*. Oxford: Butterworth-Heinemann, 1986.

[51] J. Rest, Y. S. Kim, G. L. Hofman, M. K. Meyer, and S. L. Hayes, “U-Mo Fuels Handbook,” 2009.

7 NOMENCLATURE

A	Area
A	Extensional Stiffness
B	Stiffness Parameter
C	Stiffness Parameter
D	Flexural Rigidity
D_{mon}	Flexural Rigidity Monocoque Analogy
D_{IL}	Flexural Rigidity Ideal Laminate Model
d	Plate Depth
E	Young's Modulus
E_{IR}	Young's Modulus Inner Region
E_{OR}	Young's Modulus Inner Region
g	Acceleration of Gravity
h	Flow Channel Height
I	Second Area Moment of Inertia
k	Indicating k-th Layer
k	Edge Boundary Constant
L	Span Width
M	Moment Couple
N	Force Resultant
P	Load
P	Pressure
Q	Stiffness Parameter
q	Dynamic Pressure
q_{cr}	Critical Dynamic Pressure
t	Time
t	Thickness
t_{IR}	Thickness Inner Region
t_{OR}	Thickness Outer Region
u	Displacement
v	Fluid Velocity
v_{cr}	Critical Fluid Velocity
x	Cartesian Direction
y	Cartesian Direction
y	Deflection

z	Cartesian Direction
z	Height
z	Position From Centerline in a Sandwich Structure
ϑ	Specific Energy
ς	Internal Energy
$\bar{u}^2/2$	Kinetic Energy
σ	Stress
ε	Strain
κ	Curvature

8 APPENDIX A: CRITICAL FLOW VELOCITY DERIVATION

This appendix shows the derivation of critical flow velocity and critical dynamic pressure for the case with both edges simply supported and on edge simply supported to and one clamped. This section outlines the derivation of these methods briefly, because many key details can be found in the "Model and Methods" section above.

It is important to note that the case with both edges simply supported is statically determinate and the case with one edge clamped and one simply supported is statically indeterminate.

The Euler-Bernoulli beam equation for a beam undergoing small deflections is shown in equation (3.1). Where D is the flexural rigidity, $P(x)$ is the distributed load on the beam, y is the out of plane deflection, and x is in reference to the span- width of the beam.

$$D\frac{d^4y}{dx^4} = P(x) \tag{3.1}$$

Solving equation (3.1) for the case with both edges simply supported yields equation (8.1) [17].

$$y = \frac{P}{24D}\left(x^4 - 2Lx^3 + L^3x\right) \tag{8.1}$$

Solving equation (3.1) for the case with one edge simply supported and one edge clamped yields equation (8.2) [28].

$$y = \frac{P}{24D}\left(x^4 - \frac{5}{2}Lx^3 + \frac{3}{2}L^2x^2\right) \tag{8.2}$$

Two times the integration of equation (8.1) or (8.2), divided by the original flow are $A_0 = Lh$ yields a relation for the relative change in flow area for a pair of plates.

The relative change in flow area for a pair of plates, for the case with both edges simply supported is shown in equation (8.3).

$$\frac{\Delta A}{A_0} = \frac{PL^4}{60Dh} \tag{8.3}$$

The relative change in flow are for a pair of plates, for the case with one edge simply supported and the other clamped is shown in equation (8.4).

$$\frac{\Delta A}{A_0} = \frac{PL^4}{160Dh} \tag{8.4}$$

From this point on the hydraulic domain must be derived. This portion of the derivation is identical to the derivation of the hydraulic domain in the models and methods section. For the sake of brevity, this derivation is not shown in detail in this appendix. Solving the hydraulic domain, yields the following relation for the hydraulic domain.

$$\Delta P = 2\rho v_o^2 \Delta A \left(A_o\right)^{-1} \tag{3.15}$$

Inputting equation (8.3) into equation (3.15) and solving for velocity, yields the critical flow velocity for a pair of plate with both edges simply supported which is shown in equation (8.5).

$$V_{cr} = \left(\frac{h}{\rho L^4}\right)^{1/2} \left(30D\right)^{1/2} \tag{8.5}$$

Inputting equation (8.4) into equation (3.15) and solving for velocity, yields the critical flow velocity for a pair of plate with one edge simply supported and the other clamped which is shown in equation (8.6).

$$V_{cr} = \left(\frac{h}{\rho L^4} \right)^{1/2} (80D)^{1/2} \tag{8.6}$$

The critical dynamic pressure can be found by inputting critical flow velocity into the dynamic pressure equation and multiplying by two.

The critical dynamic pressure for the case with both edges simply supported is shown in equation (8.7).

$$q_{cr} = \left(\frac{h}{L^4} \right) (30D) \tag{8.7}$$

The critical dynamic pressure for the case with one edge simply supported and the other clamped is shown in equation (8.8).

$$q_{cr} = \left(\frac{h}{L^4} \right) (80D) \tag{8.8}$$

9 APPENDIX B: THE PARALLEL AXIS THEOREM

It is interesting to note, that the monocoque flexural rigidity can be simultaneously obtained by applying the parallel axis theorem to the simplified sandwich beam shown in Figure 3-5. This section is only meant to aid the users understanding of the monocoque analogy, while section 3.2.1 above derives the monocoque analogy from a general stress state (i.e. first principles).

Application of the parallel axis theorem to sandwich structures has been referred to as a "good starting point" or "back of the envelope" method by many authors [22],[45]. As above the contribution of the outer regions is considered, while the contribution of the inner region is ignored. This is shown below.

$$D = \frac{E\bar{I}}{\left(1-\nu^2\right)} \tag{9.1}$$

$$I_x = \int_A y^2 da \tag{9.2}$$

$$I_x = \overline{I_{x'}} + Ad^2 \tag{9.3}$$

Equation (9.1) is the general form that the flexural rigidity will take in this case. Equation (9.2) is the rote definition of the parallel axis theorem [17], for a Cartesian system. Equation (9.3) is the parallel axis theorem expanded for a rectangular beam. The $\overline{I_{x'}}$ term is the second are moment of inertia, of an individual component of the sandwich beam with respect to the centroid of the beam. As discussed the sandwich structure derives most of its stiffness from the outer regions, by increasing the distance between corresponding outer regions. Thus the single component $\overline{I_{x'}}$ term for the outer regions is unimportant, and can be ignored. The inner region is also ignored in the monocoque analogy, so the $\overline{I_{x'}}$ for the inner region is also ignored. The

sandwich structure, is also analyzed as having unit width, this reduces the *A* term to the thickness of the outer region. This is shown below, each *I* shown is the second area moment of inertia for either the top or bottom outer region with the simplifications mentioned above, and the *d* term is the distance from the centroid of the entire sandwich structure to the centroid of the respective outer region. Equations (9.4) and (9.5)below imply that the stiffness of a sandwich structure is most highly dependent on the term *d*.

$$I_1 = t_1 d_1^2 \tag{9.4}$$

$$I_3 = t_3 d^2 \tag{9.5}$$

$$d_1 = \frac{1}{2}\left(t_1 + t_2\right) \tag{9.6}$$

$$d_3 = \frac{1}{2}\left(t_2 + t_3\right) \tag{9.7}$$

Equation (9.4)-(9.7)can now be combined by simply summing the inertia terms. This will yield $\bar{I}$.

$$\bar{I} = I_1 + I_2 \tag{9.8}$$

$$\bar{I} = \frac{t_1}{2}\left(t_1 + t_2\right)^2 + \frac{t_3}{2}\left(t_2 + t_3\right)^2 \tag{9.9}$$

Assuming the sandwich is symmetric, isotropic, and the outer regions are of equal thickness will yield the monocoque analogy. Equations (9.10)-(9.13) restate this information and the constants used in this derivation.

$$t_{OR} = t_1 = t_3 \tag{9.10}$$

$$t_{IR} = t_2 \tag{9.11}$$

$$E_{OR} = E_1 = E_3 \tag{9.12}$$

$$\nu_{OR} = \nu_1 = \nu_3 \tag{9.13}$$

Equation (9.14), represents the form second area moment of inertia takes when inputting the information from equations (9.10)-(9.13).

$$\bar{I} = \frac{t_{OR}}{2}\left(t_{IR} + t_{OR}\right)^2 \tag{9.14}$$

Combing equation (9.1) and (9.14), yields the monocoque analogy derived from using the parallel axis theorem.

$$D_{mon} = \frac{E}{\left(1-\nu^2\right)}\bar{I} \tag{9.15}$$

$$D_{mon} = \frac{\left(t_{IR} + t_{OR}\right)^2 t_{OR}}{2}\frac{E_{OR}}{\left(1-\nu_{OR}^2\right)} \tag{3.24}$$

10 APPENDIX C: TEST CASE 3-ADDITIONAL INFORMATION

The work presented in Test Case 3 is now expanded by exploring how changes in each layers material composition effects the Ideal Laminate model as the thickness of the inner region relative to the outer region is changed.

Figure 10-1 compares the ratio of critical velocities to the ratio of Young's Moduli as the inner region thickness is varied from 1 percent to 100 percent of the total sandwich thickness. Young' modulus is varied from 1E-1 to 1E1, all other inputs are the same as those presented in Test Case 3

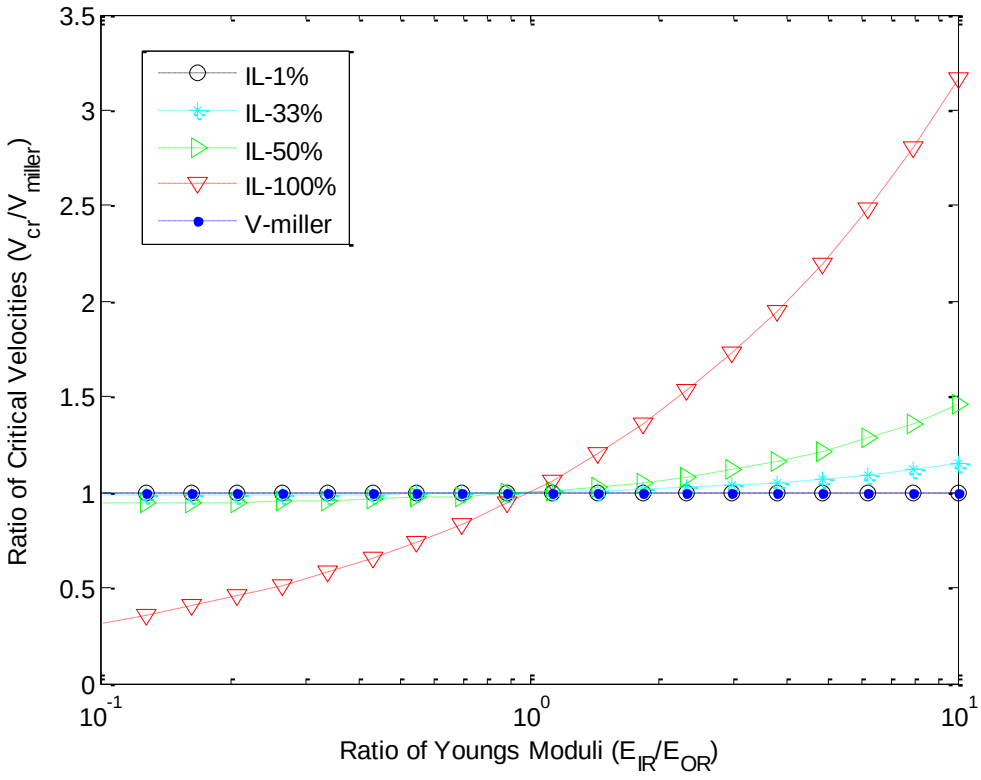

Figure 10-1: Critical velocity ratio vs. Young's Moduli ratio and thickness

Figure 10-2 compares the ratio of critical velocities, the ratio of Young's Moduli, and the percentage of the sandwich thickness that is the total thickness for the ideal

laminate case. The ratio of Young's Moduli is varied from 1E-1 to 1E1, all other inputs are the same as those presented in Test Case 3.

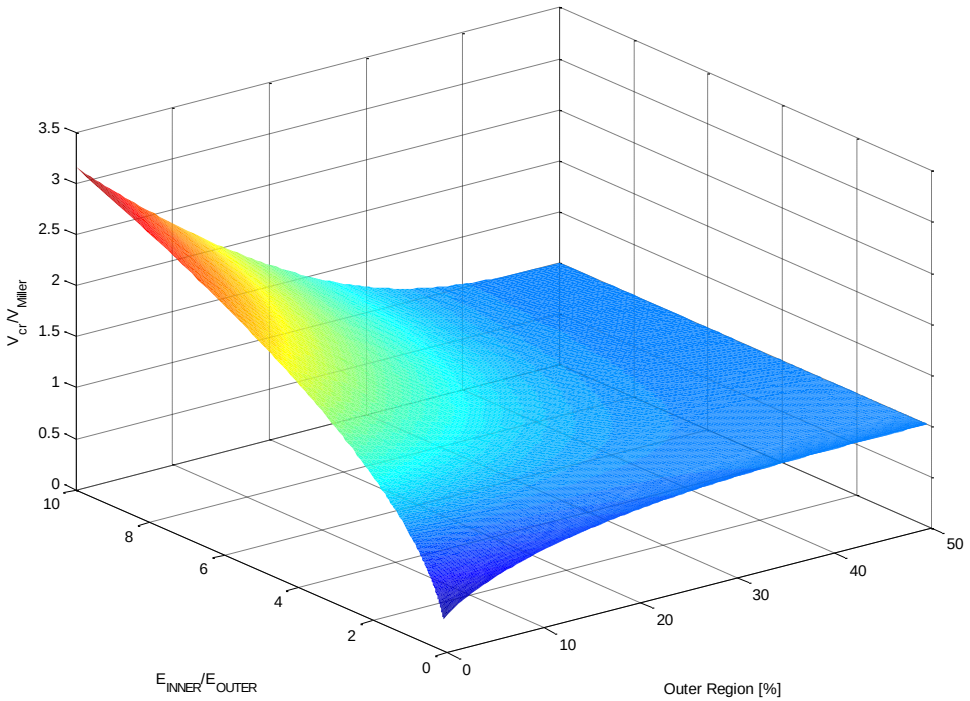

Figure 10-2: Ratio critical velocities, Young's Moduli, & region thickness

11 APPENDIX D: NON-NORMALIZED PLOTS

Test Case-1 and Test Case-3, presented a normalized plot featuring the ratio of critical velocities. In this appendix the non-normalized plots are presented.

Test Case-1 non-normalized is presented below in Figure 11-1. It compares the critical flow velocity to the percentage that is represented by the inner region thickness. The plot inputs are the same as those presented in Test Case-1.

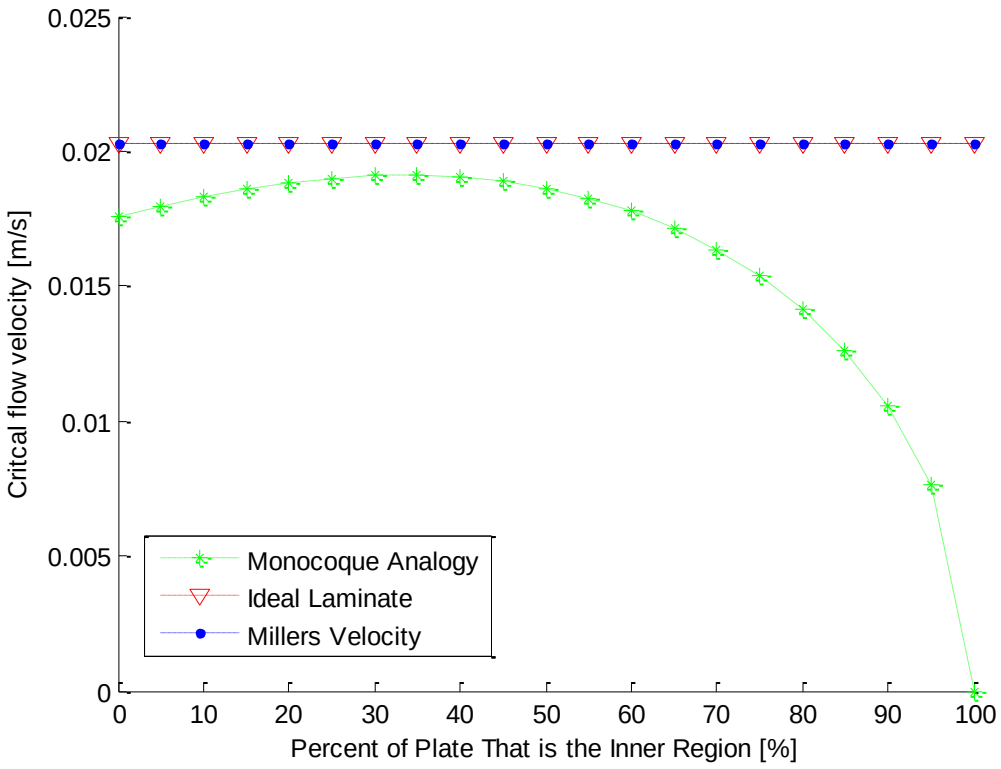

Figure 11-1: Test Case-1 non-normalized

Test Case-3 non-normalized is presented in Figure 11-2. It compares the critical flow velocity to the ratio of Young's Moduli. The plots inputs are the same as those presented in Test-Case-3.

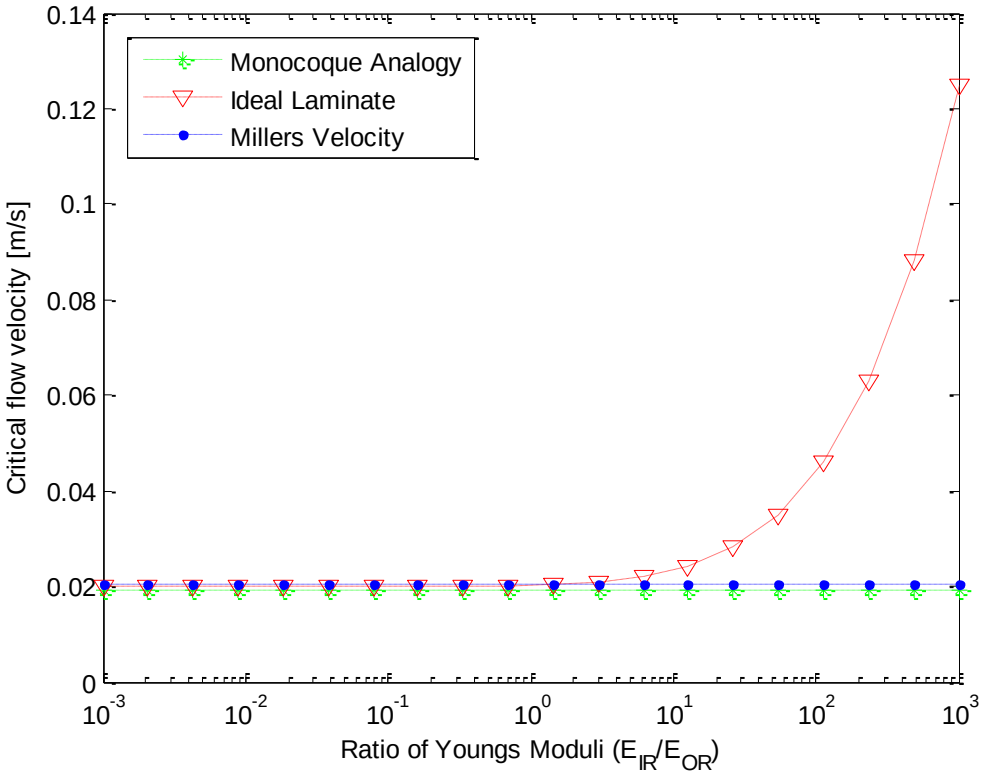

Figure 11-2: Test Case-3 non-normalized